CORE
Metadata, citation and similar papers at core.ac.uk
Provided by Texas A&M Repository

ANALYSIS OF CODED OFDM SYSTEM OVER FREQUENCY-SELECTIVE FADING CHANNELS

A Thesis

by

JUN ZHENG

Submitted to the Office of Graduate Studies of
Texas A&M University
in partial fulfillment of the requirements for the degree of

MASTER OF SCIENCE

August 2003

Major Subject: Electrical Engineering

ANALYSIS OF CODED OFDM SYSTEM

OVER FREQUENCY-SELECTIVE FADING CHANNELS

A Thesis

by

JUN ZHENG

Submitted to Texas A&M University
in partial fulfillment of the requirements
for the degree of

MASTER OF SCIENCE

Approved as to style and content by:

Scott L. Miller (Chair of Committee)	
Krishna R. Narayanan (Member)	Andrew K. Chan (Member)
Joseph D. Ward (Member)	Chanan Singh (Head of Department)

August 2003

Major Subject: Electrical Engineering

ABSTRACT

Analysis of Coded OFDM System
over Frequency-Selective Fading Channels. (August 2003)
Jun Zheng, B.S., Tsinghua University, P.R. China
Chair of Advisory Committee: Dr. Scott L. Miller

This thesis considers the analysis of system performance and resource allocation for a coded OFDM system over frequency selective fading channels. Due to the inseparable role taken by channel coding in a coded OFDM system, an information theoretical analysis is carried out and taken as the basis for the system performance and throughput.

Based on the results of the information theoretical analysis, the optimal system BER performance of a coded OFDM system is first shown to converge to the outage probability for large OFDM block lengths. Instead of evaluating the outage probability numerically, we provide in this thesis a simple analytical closed form approximation of the outage probability for a coded OFDM system over frequency selective quasi-static fading channels. Simulation results of the turbo-coded OFDM systems further confirm the approximation of the outage probability.

By taking the instantaneous channel capacity as the analytical building block, system throughput of a coded OFDM system is then provided. With the aim to compare the performance difference between adaptive and uniform resource allocation strategies, the system throughput of different allocation schemes under various channel conditions is analyzed. First, it is demonstrated that adaptive power allocation over OFDM sub-carriers at the transmitter achieves very little gain in terms of throughput over a uniform power distribution scheme. Theoretical analysis is then

provided of the throughput increase of adaptive-rate schemes compared with fixed-rate schemes under various situations. Two practical OFDM systems implementing rate-compatible-punctured-turbo-code-based (RCPT-based) hybrid automatic-repeat-request (Hybrid-ARQ) and redundancy incremental Hybrid-ARQ protocols are also provided to verify the analytical results.

To my Mom, Jinhua

ACKNOWLEDGMENTS

I would like to thank my advisor, Dr. Scott L. Miller, for his inspirational guidance, constant support and encouragement throughout my thesis work. He instilled in me the knowledge required for a master's degree and an understanding of research philosophy and ability critical to an independent researcher. I am also thankful to my committee members, Dr.Krishna R. Narayanan, Dr. Andrew K. Chan, and Dr. Joseph D. Ward for their valuable comments and time.

I also want to take this opportunity to recognize all my colleagues in the Wireless Communication Lab of Texas A&M University, especially Dr. Yu Zhang, Yan Wang, Dr. Zhongmin Liu, Dr. Zigang Yang, Guosen Yue, Xuechao Du, Hui Liu, Guang Zeng, Wenyan He, Yongzhe Xie, Peiris Janath, Shi Kai, Yong Sun and Jianping Hua, for the encouragement and insightful discussions.

TABLE OF CONTENTS

CHAPTER		Page
I	INTRODUCTION	1
	A. OFDM and Coded OFDM	1
	B. Performance Analysis of Coded OFDM Systems	1
	C. Resource Allocation for Coded OFDM Systems	3
II	SYSTEM MODEL	5
	A. Time Domain OFDM System Model	5
	B. Equivalent Frequency Domain Coded OFDM System Model	6
III	INFORMATION THEORETICAL ANALYSIS	9
	A. The Concept of Instantaneous Channel Capacity	9
	B. Examples of Instantaneous Capacity	12
IV	PERFORMANCE ANALYSIS OF CODED OFDM SYSTEMS	15
	A. Outage Probability and System Performance	15
	B. Approximation of the Outage Probability	16
	C. Numerical and Simulation Results	18
	1. Upper Bounds and Lower Bounds	18
	2. Outage Probability	20
	3. Results of Practical Codes	20
	D. Conclusion on Performance Analysis	22
V	RATE AND POWER ALLOCATION OF CODED OFDM SYSTEMS	24
	A. Assumption on Channel State Information	24
	B. Adaptive-Modulation	24
	C. Power Allocation	25
	D. Rate Allocation	32
	E. Practical Schemes	40
	F. Throughput Analysis of Practical Schemes	44
	G. Simulation Results	47
	H. Conclusion on Resource Allocation	50

Page

VI SUMMARY 53

A. Performance Analysis of Coded OFDM Systems 53
B. Rate and Power Allocation of Coded OFDM Systems . . . 53

REFERENCES 55

APPENDIX A 59

APPENDIX B 61

VITA 64

LIST OF TABLES

TABLE Page

I Puncturing tables for the RCPT code with puncturing period $p = 4$ and information block size $N = 1024$ 48

LIST OF FIGURES

FIGURE		Page
1	Time domain OFDM system model	5
2	Frequency domain OFDM system model	7
3	Approximation of the conditional sub-channel capacity for binary input soft output channel	13
4	Random coding upper bound and the strong converse lower bound as well as the approximated outage probability for a coded OFDM system with $N = 1024$ subcarriers over a frequency-selective fading channel with $L = 1, 2, 3$ paths	18
5	Upper and lower bounds for three coded OFDM systems of different numbers of subcarriers, $N = 1024, 256, 64$, transmitted over frequency-selective fading channels with $L = 2$ paths	19
6	Exact outage probability vs. the approximated outage probability for a coded OFDM system with $N = 1024$ subcarriers over a frequency-selective fading channel with $L = 2 \sim 9$ paths	20
7	Block error probability of a rate 1/2 terminated convolutional code with constraint length $K = 9$ and generator polynomial $(561, 753)$ compared with the approximated outage probability . . .	21
8	Block error probability of a rate 1/2 turbo code with component generator polynomial $(7, 5)$ compared with the approximated outage probability	22
9	Throughput comparison between the water-filling power allocation and the uniform power allocation (for unconstrained input and soft output channels)	32
10	Ultimate throughput gain of the water-filling power allocation over the uniform power allocation (for unconstrained input and soft output channels)	33

FIGURE Page

11 Throughput comparison between the water-filling power allocation and the uniform power allocation (for binary input and soft output channels) 34

12 Ultimate throughput gain of the water-filling power allocation over the uniform power allocation (for binary input and soft output channels) 35

13 PDF of the instantaneous channel capacity 36

14 Histogram of the instantaneous channel capacity for an OFDM system with 1024 sub-carriers, and $L = 2, 5, 10, 40, 100$ independent fading paths 36

15 Ideal throughput comparison between the rate-adaptive schemes and the rate-fixed schemes (under the condition of perfect coding and infinite available code rates) 39

16 Rate compatible punctured turbo (RCPT) encoder 41

17 Simulation throughput for Hybrid-ARQ (Type I) and redundancy incremental Hybrid-ARQ (Type II) OFDM systems 49

18 Simulation throughput gain for Hybrid-ARQ (Type I) and redundancy incremental Hybrid-ARQ (Type II) OFDM systems 50

19 Simulation throughput for Hybrid-ARQ (Type I) and redundancy incremental Hybrid-ARQ (Type II) OFDM systems under different fading rates (normalized Doppler frequency $f_d T_{frame} = 10^{-2}, 10^{-3}$) 51

20 Performance analysis of the throughput for Hybrid-ARQ (Type I) and redundancy incremental Hybrid-ARQ (Type II) OFDM systems 52

CHAPTER I

INTRODUCTION

In this chapter, we are going to take an overview of the background information with the aim to provide an intuitive explanation of our research motivation.

A. OFDM and Coded OFDM

Orthogonal frequency-division multiplexing (OFDM) has recently received increased attention due to its capability of supporting high-data-rate communication in frequency selective fading environments which cause inter-symbol interference (ISI) [1][2]. Instead of using a complicated equalizer as in the conventional single carrier systems, the ISI in OFDM can be eliminated by adding a guard interval which significantly simplifies the receiver structure. However, in order to take advantage of the diversity provided by the multi-path fading, appropriate frequency interleaving and coding is necessary. Therefore, coding becomes an inseparable part in most OFDM applications and a considerable amount of research has focused on optimum encoder, decoder, and interleaver design for information transmission via OFDM over fading environments, e.g. [3]-[6].

B. Performance Analysis of Coded OFDM Systems

Although a considerable amount of research has addressed the design and implementation of coded OFDM systems for frequency-selective fading channels, comparatively few of them provide satisfactory performance analysis of such systems because of the complicated nature of this problem. Here we consider a frequency-selective quasi-

---

The journal model is *IEEE Transactions on Automatic Control*.

static fading channel, which is a reasonable assumption for an indoor wireless environment that has multipath fading but exhibits very slow changes over time, modeled as quasi-static. Unlike coding in AWGN channels, where there is one dominant pairwise error probability, related to the minimum distance of a block code or the free distance of a convolutional code, that determines the system performance, all pairwise error probabilities in a fading coded OFDM system decrease as inverse polynomial of the signal-to-noise ratio (SNR). Thus the powerful union-Chernoff bound will be too loose at any range of SNR when the block length is large.

Motivated by the performance analysis results on block fading channels in [7], the random coding upper bounds [8] [9] and the strong converse lower bounds [10] as well as the concept of instantaneous channel capacity are implemented for the performance analysis of coded OFDM system. Both the upper bounds and lower bounds are shown to converge to the channel outage probability for large OFDM block lengths, and hence we focus our primary attention on the channel outage probability and take it as the theoretical achievable performance indicator for the coded OFDM system. Instead of evaluating the outage probability numerically, a much more simple analytical closed form approximation of the outage probability is provided in this thesis. Starting from the capacity approximation of the binary input alphabet channel, the outage probability for a coded OFDM system over frequency-selective fading channels is approximated and simplified to a analytically tractable form. Simulation results of the real outage probability as well as the performance of a practical turbo-coded OFDM system further confirms the fitness of this approximation.

C. Resource Allocation for Coded OFDM Systems

All of the above work is based on the assumption that only the receiver has channel state information (CSI). If information is allowed to flow in the other direction, so that the transmitter and the receiver share all or part of the channel state information, adaptive power and code rate allocation within the OFDM system becomes possible and is expected to achieve significant performance gain. Several adaptive schemes for OFDM systems have been investigated in [11]-[16]. Ditzel and Serdijn [11] proposes an optimal energy allocation scheme among different OFDM sub-carriers which minimizes the total energy necessary to achieve a desired average bit error rate over frequency-selective fading channels. Using this optimal scheme, a $4dB$ performance gain is attained with respect to uniform power allocation schemes for the same system. In [12], Czylwik introduces an adaptive modulation scheme for the individual sub-carriers in an OFDM system, and the required signal to noise ratio for certain bit error probabilities is reduced dramatically compared to fixed modulation. Similar adaptive modulation schemes, recommended by Maeda et al. in [13], implement the idea of puncturing codes to delete code bits in non-reliable sub-carriers in an OFDM frame, hence suppressing the total power consumption. Recent research work [14] [15] focuses on joint power, code rate, and modulation allocation among OFDM sub-carriers and achieves comparable performance gains with respect to uniform resource allocation. Piazzo [16] also provides a fast and convergent algorithm on the adaptive power and bit allocation in OFDM systems, which proves to be useful when the channel is changing rapidly. However, most of these approaches focus on uncoded OFDM (or systems with very weak codes) which fails to take advantage of the significant advances that have been made in coding for error correction and detection.

In this thesis, transmitter power and code rate allocations for a coded OFDM

system over frequency-selective fading channels have been analyzed. The channel state information is assumed to be accessible to both the transmitter and the receiver, which is not a stringent constraint in most wireless communication systems where there exists a reverse link. Different from previous uncoded OFDM systems, coding plays an important part in maintaining reliable communication between the transmitter and receiver in our study. It is then reasonable to analyze the adaptive schemes from an information theoretical point of view, when powerful channel coding techniques such as turbo codes or LDPC codes are implemented in the system. Starting from channel capacity analysis, the concept of instantaneous channel capacity is again implemented as the building block for the system analysis. The theoretical throughput for the OFDM system under optimal power and rate allocations among different OFDM sub-carriers is provided and taken as the ultimate system performance limit for any practical application. Various analyses are carried out on different channel models and fading environments, and compared with the uniform power and fixed rate allocation schemes respectively. In order to complement the analytical results as well as compare with the performance limit, two practical OFDM communication systems are proposed. Their performance analyses are also provided and compared with the simulation results.

CHAPTER II

SYSTEM MODEL

A. Time Domain OFDM System Model

In order to understand the mathematical principles of OFDM systems, let us first take an overview of the time domain uncoded OFDM system model, which is shown in Fig. 1.

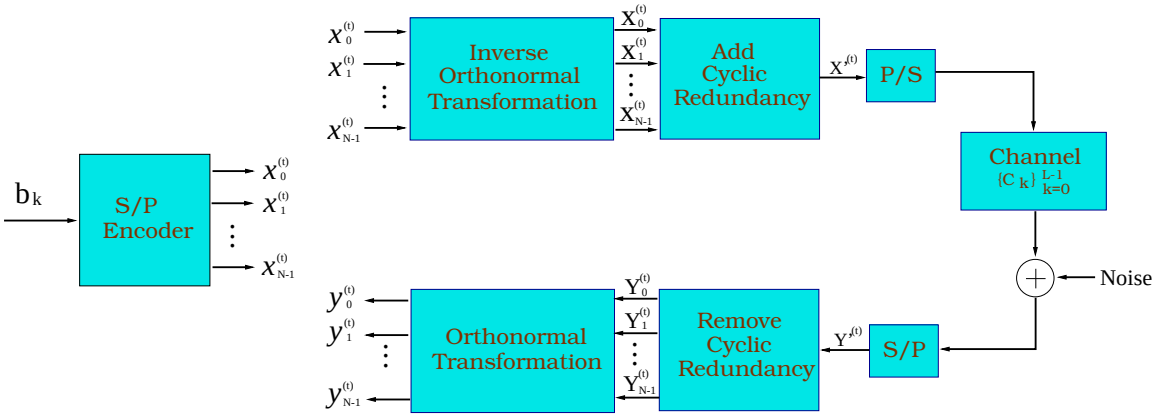

Fig. 1. Time domain OFDM system model

Let b_k represent the binary data sequence to be transmitted over the channel. This data is divided into non-overlapping blocks of $n = N \cdot \log_2 M$ bits. The n bits of data are partitioned into N groups, with each $\log_2 M$ bits mapped into a complex symbol of constellation size M. Symbol $x_k^{(t)}$ is the signal transmitted over the k-th subcarrier during the t-th OFDM frame. At the transmitter, an inverse discrete Fourier transform (IDFT) is performed as a method of modulation, which results in samples $X_k^{(t)}$ given by

$$X_k^{(t)} = \frac{1}{\sqrt{N}} \sum_{i=0}^{N-1} x_i^{(t)} \cdot \exp(j\frac{2\pi ki}{N}), \quad 0 \le i \le N-1 \ . \tag{2.1}$$

Assume that the channel is frequency-selective, and hence the implementation of a cyclic redundancy of sufficient length to the N-point OFDM frame is an effective method to counter intersymbol interference (ISI) caused by the channel. The cyclic prefix causes the sequence $\{X_k^{(t)}\}$ to appear periodic to the channel and clears the channel memory at the end of each OFDM frame. This action makes successive transmissions independent. The output from the channel, with additive noise $N_k^{(t)}$, may be written as

$$Y_k^{(t)} = c_k^{(t)} \star X_k(t) + N_k^{(t)}, \tag{2.2}$$

where $c_k^{(t)}$ is the discretized fading channel coefficient.

At the receiver, the cyclic prefix is discarded to obtain a frame of N symbols $Y_k^{(t)}$. Taking the N-point discrete Fourier transform of the received samples $Y_k^{(t)}$, we have the output samples given by

$$y_k^{(t)} = \frac{1}{\sqrt{N}} \sum_{i=0}^{N-1} Y_i^{(t)} \cdot \exp(-j\frac{2\pi ki}{N}), \quad 0 \le i \le N-1 \ . \tag{2.3}$$

B. Equivalent Frequency Domain Coded OFDM System Model

Although the time domain model provided in the previous section is conceptually straightforward, it is much more insightful to analyze the OFDM system in the frequency domain since the information symbols modulate different subcarriers in the frequency domain. Hence, let us consider the frequency model for a coded OFDM system illustrated in Fig. 2. A block of k information bits, denoted as $\mathbf{b} = (b_1, \cdots, b_k)$, is encoded into a codeword $\mathbf{x} = (x_1, \cdots, x_n)$ of length n, where each symbol x_i is an element from a complex alphabet $\mathcal{X}$. There are a total of m codewords in the code book and the code rate is defined to be $R = (\log_2 m)/n$. Note that here we combine encoder, modulator, and interleaver together to form one super encoder E.

The encoded block $\mathbf{x} = (x_1, \cdots, x_n)$ is segmented into l frames, each of length

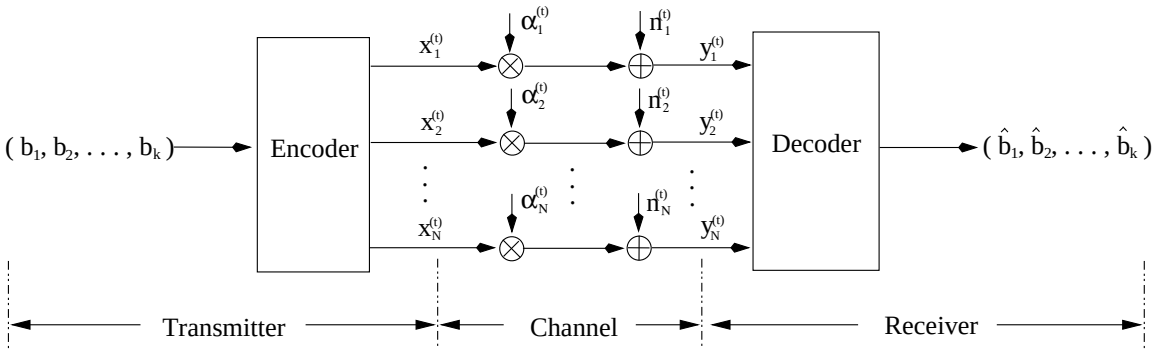

Fig. 2. Frequency domain OFDM system model

$N(lN = n)$. The individual frame is transmitted by N dependent parallel sub-channels, each representing a different OFDM sub-carrier. According to the tapped-delay-line model [17], the fading coefficients $\alpha_i^{(t)}$ of the t^{th} OFDM frame are related to the fading envelopes $c_i^{(t)}$ through

$$\mathbf{c}^{(t)} = [\, c_1^{(t)}, \cdots, c_L^{(t)}, 0, \cdots, 0 \,]^T \in \mathcal{C}^{N\times 1}, \tag{2.4}$$

$$\boldsymbol{\alpha}^{(t)} = [\, \alpha_1^{(t)}, \cdots, \alpha_N^{(t)} \,]^T \in \mathcal{C}^{N\times 1}, \tag{2.5}$$

$$\boldsymbol{\alpha}^{(t)} = W_{N\times N}\mathbf{c}^{(t)} \ , \tag{2.6}$$

where the Fourier transformation $W_{N\times N}$ is given by

$$W_{N\times N} = \begin{pmatrix} w^0 & w^0 & \dots & w^0 \\ w^0 & w^1 & \dots & w^{N-1} \\ w^0 & w^2 & \dots & w^{2(N-1)} \\ \vdots & \vdots & \vdots & \ddots \\ w^0 & w^{N-1} & \dots & w^{(N-1)(N-1)} \end{pmatrix}, \ w = e^{-j\frac{2\pi}{N}} \ . \tag{2.7}$$

We can further stack l consecutive fading coefficients and envelopes into a compact vector form as

$$\mathbf{c} = [\,{\mathbf{c}^{(1)}}^T, \cdots, {\mathbf{c}^{(l)}}^T\,]^T \in \mathcal{C}^{n\times 1}, \tag{2.8}$$

$$\boldsymbol{\alpha} = [\,{\boldsymbol{\alpha}^{(1)}}^T, \cdots, {\boldsymbol{\alpha}^{(l)}}^T\,]^T \in \mathcal{C}^{n\times 1}, \tag{2.9}$$

where the fading envelope $\mathbf{c}^{(t)}$ is assumed to be constant within one OFDM frame, but is a function of time t from frame to frame. Each component $c_i^{(t)}$ of the fading envelope is assumed to be independent from tap to tap. A Rayleigh fading distribution is considered in this paper with the probability density function (pdf) of $|c_i^{(t)}|$ given by

$$f_{|c_i^{(t)}|}(x) = \frac{x}{\sigma^2}\exp(-x^2/2\sigma^2), \qquad x \geq 0, \tag{2.10}$$

where $E[|c_i^{(t)}|^2] = 2\sigma^2$ is the average power of the fading envelope. It is further assumed that each tap has the same average power (this model can be generalized to have non-uniform power delay profile).

The received output vectors $\mathbf{y}^{(t)}$ are given by

$$\mathbf{y}^{(t)} = [\,y_1^{(t)}, y_2^{(t)}, \cdots, y_N^{(t)}\,]^T, \qquad (1 \leq t \leq l) \tag{2.11}$$

$$y_i^{(t)} = \alpha_i^{(t)} x_i^{(t)} + n_i^{(t)}, \qquad (1 \leq i \leq N) \tag{2.12}$$

where additive complex Gaussian noise $n_i^{(t)}$ is white with variance N_0. The receiver is assumed to have perfect knowledge of the channel state information (CSI) and makes decisions based on the observation of the received vector $\mathbf{y}^{(t)}, 1 \leq t \leq l$, and the channel state information $\mathbf{c}$.

CHAPTER III

INFORMATION THEORETICAL ANALYSIS

In this chapter, analysis taken from an information theoretical perspective is provided as the buildingblocks for the coded OFDM system analysis.

A. The Concept of Instantaneous Channel Capacity

The well known Shannon capacity theory states that we can send information with arbitrarily low error probability as long as the rate in bits per channel use is less than the channel capacity [18]. But this capacity is achieved upon coding over time with an infinite or huge codeword length. In coded OFDM systems, coding is performed in the frequency domain instead of the time domain, where only a limited number of OFDM frames are taken to form one codeword. Thus the maximum achievable information rate or the channel capacity of a coded OFDM system and its relationship with the conventional channel capacity of an AWGN channel presents an interesting research problem.

Using the techniques introduced in [19], via slight modifications, we can obtain the random coding upper bound (see, e.g., [8], and [9]) and the strong converse lower bound (see, e.g., [9], and [10]) for the OFDM system introduced in Chapter II.

$$\overline{P_e(\boldsymbol{\alpha})} \leq \begin{cases} 2^{-n\left(\frac{1}{p}\sum_{t=1}^{p} E_N(R|\boldsymbol{\alpha}^{(t)})\right)}, & \text{for } 0 \leq R < C_n(\boldsymbol{\alpha}) \ , \\ 1, & \text{for } R \geq C_n(\boldsymbol{\alpha}) \ , \end{cases} \tag{3.1}$$

$$P_c(\boldsymbol{\alpha}) \leq \begin{cases} 2^{-n\left(\frac{1}{p}\sum_{t=1}^{p} E_N^{SC}(R|\boldsymbol{\alpha}^{(t)})\right)}, & \text{for } R \geq C_n(\boldsymbol{\alpha}) \ , \\ 1, & \text{for } 0 \leq R < C_n(\boldsymbol{\alpha}) \ , \end{cases} \tag{3.2}$$

where

$$E_N(R|\boldsymbol{\alpha}^{(t)}) = \max_{0\le\rho\le 1}\Big[\max_{q^{(t)}}\frac{1}{N}\sum_{i=1}^{N}E_0(\rho, q_i^{(t)}|\alpha_i^{(t)}) - \rho R\Big]\ , \tag{3.3}$$

$$E_N^{SC}(R|\boldsymbol{\alpha}^{(t)}) = \max_{-1\le\rho\le 0}\Big[\min_{q^{(t)}}\frac{1}{N}\sum_{i=1}^{N}E_0(\rho, q_i^{(t)}|\alpha_i^{(t)}) - \rho R\Big]\ , \tag{3.4}$$

$$E_0(\rho, q_i^{(t)}|\alpha_i^{(t)}) = -\log_2\left\{\sum_{y_i^{(t)}}\Big[\sum_{x_i^{(t)}} q_i^{(t)}(x_i^{(t)})p(y_i^{(t)}|x_i^{(t)}, \alpha_i^{(t)})^{1/(1+\rho)}\Big]^{1+\rho}\right\}, \tag{3.5}$$

and

$$C_n(\boldsymbol{\alpha}) = \frac{1}{l}\sum_{t=1}^{l}C_N(\boldsymbol{\alpha}^{(t)})\ , \tag{3.6}$$

where

$$C_N(\boldsymbol{\alpha}^{(t)}) = \frac{1}{N}\max_{q^{(t)}} I(\mathbf{x}^{(t)};\mathbf{y}^{(t)}|\boldsymbol{\alpha}^{(t)}) = \frac{1}{N}\sum_{i=1}^{N}\max_{q_i^{(t)}} I(x_i^{(t)};y_i^{(t)}|\alpha_i^{(t)})\ . \tag{3.7}$$

Formula (3.1) and (3.2) describe the upper and lower bounds on the performance of a block code with rate $R = (\log_2 m)/n$. Eq. (3.1) is the upper bound of the block error probability averaged over the ensemble codebook conditioned upon the fading coefficients $\boldsymbol{\alpha}$ assuming ML decoding with perfect channel state information. Eq. (3.2) is the upper bound on the correct decoding probability for any code. From (3.1) and (3.2), we can observe that $C_n(\boldsymbol{\alpha})$ is the maximum achievable information rate in terms of bits per OFDM sub-carrier use, when the number of sub-carriers N approaches infinity. Thus, $C_n(\boldsymbol{\alpha})$ is defined to be the instantaneous channel capacity as it depends on the fading realization $\boldsymbol{\alpha}$. Formula (3.1) and (3.2) are the achievability and converse of this capacity respectively.

Note that in the above bounds, it is very difficult to optimize the distribution $q_i^{(t)}(x)$ under a generalized complex alphabet $\mathcal{X}$. However it is easy to prove that the uniform distribution is optimum when the alphabet is symmetric on the complex plane such as with M-ary PSK. Furthermore, most of the time, we are only interested

in an input alphabet that has an equal prior probability distribution. Thus the following discussion restricts the input alphabet to a uniform input distribution only. Also note that $p(y_i|x_i, \alpha_i)$ in (3.5) is a general form of the transition probability for a given sub-channel. When hard decisions are implemented at the receiver before ML detection, each sub-channel becomes a discrete symmetric channel and $p(y_i|x_i, \alpha_i)$ can be represented as

$$p = [p_1, p_2, \cdots, p_{|\mathcal{X}|}]. \tag{3.8}$$

When soft decisions are used, the transition probability can be written as

$$p(y_i|x_i, \alpha_i) = \frac{1}{\pi N_0} \exp(-\frac{|y_i - \alpha_i x_i|^2}{N_0}) \ . \tag{3.9}$$

It might be insightful to view (3.6) and (3.7) as the capacity achieved by performing independent coding over $n = lN$ independent parallel sub-channels with different signal to noise ratios determined by $\alpha_i^{(t)}$. By combining the OFDM symbols in the same sub-carrier position over a sufficient large number of OFDM frames to form one codeword, an infinite or huge decoding delay is introduced, which is intolerable in some applications. In coded OFDM, the only difference is that coding is performed in the frequency domain over a sufficiently large number of sub-carriers N, instead of coding in the time domain over a lager number of time slots and combining these n sub-channels together. In doing so, only a limited amount of decoding delay is introduced, which is tolerable in most applications. The more important issue is that we do not have to apply different alphabets or information rates for each sub-carrier due to differing signal to noise ratios. Thus it is meaningful to study the behavior of this instantaneous channel capacity.

Finally, to readers familar with block fading channels and its performance, it is no doubt helpful to make a comparison between our quasi-static fading OFDM channel

and the block fading channel in [7]. First, instead of having independent fading on different sub-channels in a block fading channel, the fading coefficients $\alpha_i^{(t)}$ of different OFDM sub-carriers are correlated. Second, even though each OFDM sub-carrier has block length 1 when viewed as a parallel block fading channel, the convergence of the upper bound and lower bound still exists for OFDM system having large number of subcarriers as is shown in the following section. This is in contrast to the convergence condition of a block fading channel (large block length).

B. Examples of Instantaneous Capacity

The simplest channel model is the Binary Symmetric Channel (BSC), where the input alphabet $\mathcal{X}$ is binary and the receiver performs hard decisions before ML detection. In this case, the sub-channel capacity conditioned on the channel coefficient $\alpha_i^{(t)}$ is given by

$$C(\gamma_i^{(t)}) = I(x_i^{(t)}; y_i^{(t)} | \alpha_i^{(t)}) = 1 - H(Q(\sqrt{2\gamma_i^{(t)}})) \ , \tag{3.10}$$

where

$$\gamma_i^{(t)} = \frac{|\alpha_i^{(t)}|^2 \cdot E_s}{N_0} \ . \tag{3.11}$$

When the demodulator forms soft decisions, the conditional sub-channel capacity is given by

$$C(\gamma_i^{(t)}) = \frac{1}{\log(2)} \Big(2\gamma_i^{(t)} - \int_{y_i} \frac{1}{4\pi\gamma_i^{(t)}} \log\Big(\cosh\left(Re[y_i]\right)\Big) \cdot \exp\big(- \frac{|y_i - 2\gamma_i^{(t)}|^2}{4\gamma_i^{(t)}}\big) \, dy_i \Big) \ . \tag{3.12}$$

If the input symbol $x_i^{(t)}$ has an unconstrained alphabet and the receiver performs soft detection, the conditional sub-channel capacity can be written as

$$C(\gamma_i^{(t)}) = \log_2(1 + \gamma_i^{(t)}) \ . \tag{3.13}$$

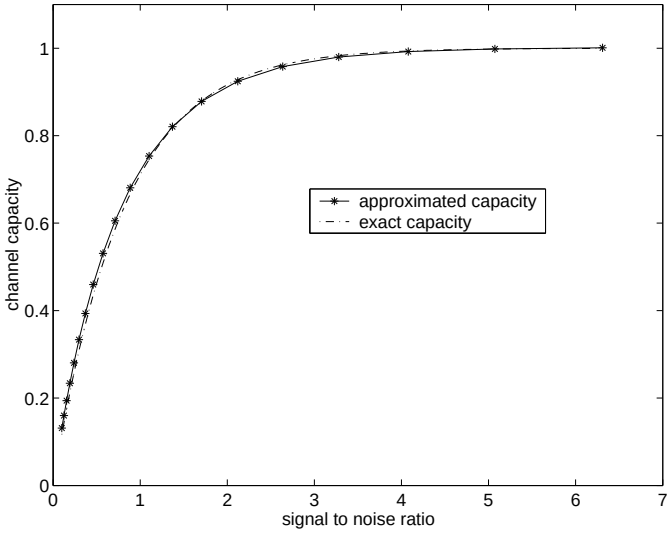

Fig. 3. Approximation of the conditional sub-channel capacity for binary input soft output channel

Using (3.6) and (3.7), the instantaneous channel capacity can be expressed as

$$C_n(\boldsymbol{\alpha}) = \frac{1}{l}\sum_{t=1}^{l} C_N(\boldsymbol{\alpha}^{(t)}) = \frac{1}{n}\sum_{t=1}^{l}\sum_{i=1}^{N} C(\gamma_i^{(t)}) \ . \tag{3.14}$$

In the following sections, a lot of attention is focused on the case of binary input soft output channels due to fact that BPSK modulation with soft output is not only conceptually simple but also widely used in practice. For the binary input soft output channel, the conditional sub-channel capacity $C(\gamma_i)$ can be well approximated by the analytically simple form

$$C(\gamma_i^{(t)}) \approx 1 - \exp(-m\gamma_i^{(t)}), \quad m = 1.24 \ . \tag{3.15}$$

The details of the derivation of this approximation are provided in Appendix A.

Results of the the exact sub-channel capacity given by (3.12) through numerical integration versus the approximation given by (3.15) are depicted in Fig. 3. From the

plot, it is seen that the exact conditional channel capacity is well approximated and almost identical to the approximated form.

CHAPTER IV

PERFORMANCE ANALYSIS OF CODED OFDM SYSTEMS

A. Outage Probability and System Performance

Based on the information theoretical analysis in the previous chapter, analytical system performance analysis is provided in this section. Here we assume each codeword is composed of only one OFDM frame ($l = 1$), and omit the superscript t in vectors $\mathbf{x}^{(t)}$, $\mathbf{y}^{(t)}$, $\mathbf{c}^{(t)}$, and $\alpha^{(t)}$. Extending the analysis to coded OFDM systems whose coding is performed on more than one OFDM frames is straightforward.

Averaging the conditional upper bound (3.1) and the lower bound (3.2) over the ensemble fading vector $\boldsymbol{\alpha}$ yields

$$\overline{P_e} = E_{\boldsymbol{\alpha}}\left[\overline{P_e(\boldsymbol{\alpha})}\right] \leq \int_{\overline{\mathcal{U}}} \left(2^{-NE_N(R/\boldsymbol{\alpha})}\right) \cdot f(\boldsymbol{\alpha})\, d\boldsymbol{\alpha} + \int_{\mathcal{U}} 1 \cdot f(\boldsymbol{\alpha})\, d\boldsymbol{\alpha}\,, \tag{4.1}$$

and

$$P_e = E_{\boldsymbol{\alpha}}\left[1 - P_c(\boldsymbol{\alpha})\right] \geq \int_{\mathcal{U}} \left(1 - 2^{-NE_N^{SC}(R/\boldsymbol{\alpha})}\right) \cdot f(\boldsymbol{\alpha})\, d\boldsymbol{\alpha} + \int_{\overline{\mathcal{U}}} 0 \cdot f(\boldsymbol{\alpha})\, d\boldsymbol{\alpha}, \tag{4.2}$$

where

$$\mathcal{U} = \{\boldsymbol{\alpha} | C_N(\boldsymbol{\alpha}) \leq R\}\ . \tag{4.3}$$

When the number of OFDM sub-carriers N is sufficient large, both the upper bound (4.1) and the lower bound (4.2) converge to the outage probability $Pr(out)$, which is defined as

$$\Pr(out) = \int_{\mathcal{U}} 1 \cdot f(\boldsymbol{\alpha})\, d\boldsymbol{\alpha} = Pr(C_N(\boldsymbol{\alpha}) \leq R)\ . \tag{4.4}$$

Since the upper bound is the ensemble average performance of all codebooks, but the lower bound is for any code, there must exists at least one coding scheme

whose performance is bounded by (4.1), (4.2) and converges to (4.4) as N goes to infinite. From now on, we will focus our attention on the outage probability, which will be used as an indicator of the system performance.

B. Approximation of the Outage Probability

When the channel is frequency selective and spread over L taps, it is quite clear from (3.12) and (3.7) that $C_N(\boldsymbol{\alpha})$ is a highly non-linear function of the vector $\boldsymbol{\alpha}$. Generally, it is very difficult to get the cdf (or pdf) of a random vector's non-linear transformation. In this paper, instead of evaluating the system performance numerically, we provide an approximate but simple analytical form for this outage probability.

Plugging (3.15) into (3.7), we have

$$C_N(\boldsymbol{\alpha}) \approx 1 - \frac{1}{N}\sum_{i=1}^{N}\exp(-m\gamma_i), \quad m = 1.24\,. \tag{4.5}$$

where γ_i is given by (3.11). If we perform a Taylor series expansion on each exponential term in the above equation, (4.5) can be written as

$$C_N(\boldsymbol{\alpha}) \approx 1 - \sum_{j=0}^{\infty}\sum_{i=1}^{N}\frac{(-m\gamma_i)^j}{N\cdot j!}. \tag{4.6}$$

Using the following fact of an exponential random variable,

$$E[\gamma_i^j] = j!\cdot E[\gamma_i]^j\,, \tag{4.7}$$

it is reasonable to extend this property from the ensemble mean to the sample mean by

$$\frac{1}{N}\sum_{i=1}^{N}\gamma_i^j \approx j!\cdot\Big(\frac{1}{N}\sum_{i=1}^{N}\gamma_i\Big)^j\,. \tag{4.8}$$

Substituting (4.8) into (4.6), the instantaneous channel capacity $C_N(\boldsymbol{\alpha})$ can be further

simplified to be

$$\begin{aligned} C_N(\boldsymbol{\alpha}) \approx \; & 1 - \sum_{j=0}^{\infty} (- m \cdot \frac{1}{N} \sum_{i=1}^{N} \gamma_i)^j \\ = \; & 1 - \frac{1}{1 + m \cdot \frac{1}{N} \sum_{i=1}^{N} \gamma_i} \; . \end{aligned} \tag{4.9}$$

Plugging (4.9) into the outage probability definition (4.4), we can get a much more simplified outage probability form

$$Pr(out) \approx Pr(\frac{1}{N} \sum_{i=1}^{N} \gamma_i \leq \frac{R}{(1-R) \cdot m}) \, . \tag{4.10}$$

According to (2.6) and (3.11), we know that the sample mean of γ_i is a quadratic transformation of $\boldsymbol{\alpha}$(or $\mathbf{c}$) given by

$$z = \frac{1}{N} \sum_{i=1}^{N} \gamma_i = \frac{1}{N} (\mathbf{c}^H W^H W \, \mathbf{c}) \frac{E_s}{N_0} = (\mathbf{c}^H \cdot \mathbf{c}) \frac{E_s}{N_0} \, . \tag{4.11}$$

From (2.10), we know that the c_i are L independent Gaussian random variables. This means that z is a central χ^2 random variable with $2L$ degree of freedom, and the outage probability is given by the cdf of this random variable

$$Pr(out) \approx 1 - \exp \big(- \frac{RL}{m(1-R)\overline{\gamma_s}} \big) \sum_{k=0}^{L-1} \frac{1}{k!} \big(\frac{RL}{m(1-R)\overline{\gamma_s}} \big)^k , \tag{4.12}$$

where

$$\overline{\gamma_s} = \frac{E_s}{N_o} \, . \tag{4.13}$$

When $\overline{\gamma_s} \gg 1$, the outage probability reduces to

$$Pr(out) \approx \frac{1}{L!} \cdot \big(\frac{RL}{m(1-R)\overline{\gamma_s}} \big)^L . \tag{4.14}$$

It is quite clear from (4.14) that the system can achieve maximum diversity order of L, which is exactly the number of paths. However, in order to achieve this maximum diversity, a powerful channel coding scheme should be implemented.

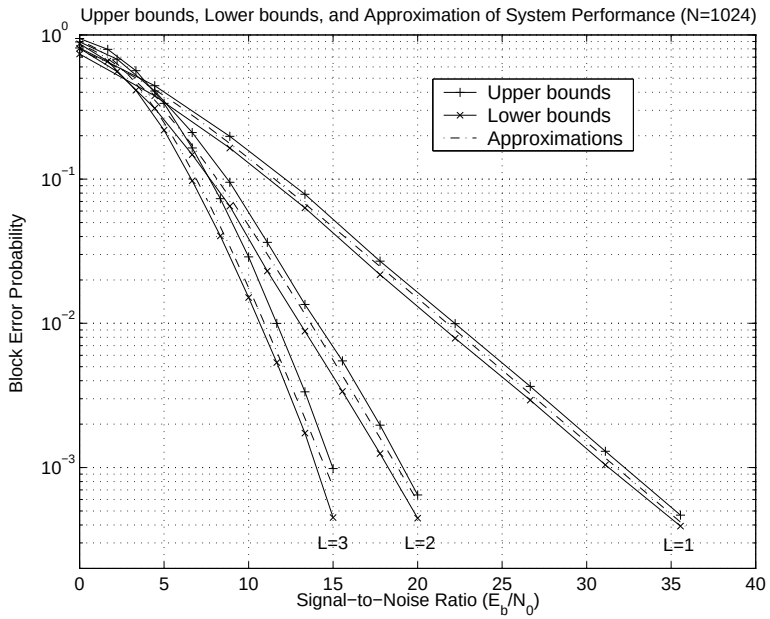

Fig. 4. Random coding upper bound and the strong converse lower bound as well as the approximated outage probability for a coded OFDM system with $N = 1024$ subcarriers over a frequency-selective fading channel with $L = 1, 2, 3$ paths

C. Numerical and Simulation Results

1. Upper Bounds and Lower Bounds

The random coding upper bound averaged over the fading coefficients based upon (3.1) and (4.1) as well as the strong converse lower bound (3.2) and (4.2) are computed numerically. We assume a binary symmetric channel model (perform hard decisions before ML detection) and a Rayleigh distribution of c_i with a rectangular multipath power profile. Results for these two bounds and the approximated outage probability are depicted in Fig. 4 for a coded OFDM system with $N = 1024$ subcarriers transmitting over a frequency-selective fading channel with several different numbers of paths.

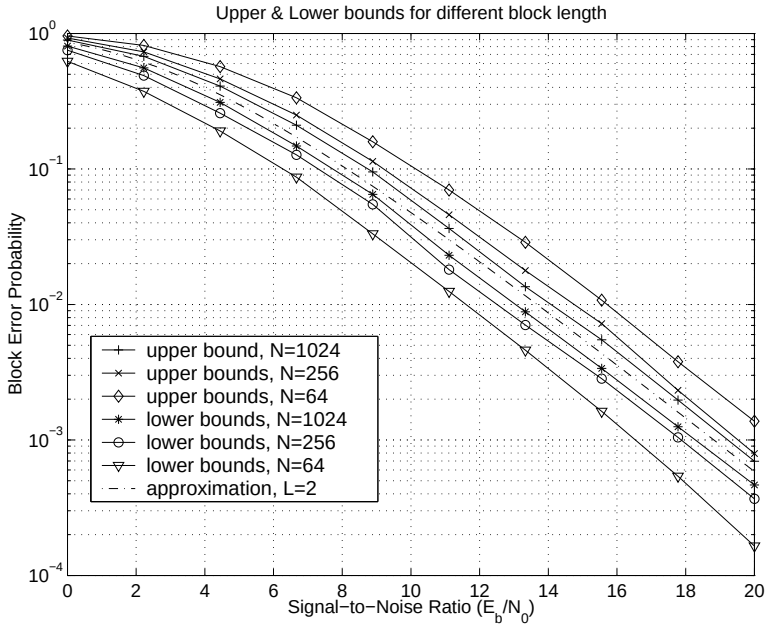

Fig. 5. Upper and lower bounds for three coded OFDM systems of different numbers of subcarriers, $N = 1024, 256, 64$, transmitted over frequency-selective fading channels with $L = 2$ paths

Theoretically, the outage probability is greater than the lower bound but less than the upper bound which is exactly the case shown in the above plot, although only an approximated result is used here. Further from Fig. 4, we see that the lower bound is only about 1dB from the upper bound, which indicates that both of these bounds and also the approximated outage probability are quite tight and a valid performance indication of the system for large block lengths.

To see the sensitivity of the tightness of the bounds in terms of the block length, we depict in Fig. 5 the bounds for the same rate $R = 1/2$ system under three different block lengths. From it, we see that the two bounds and the approximated outage probability are reasonably tight when $N \geq 256$.

2. Outage Probability

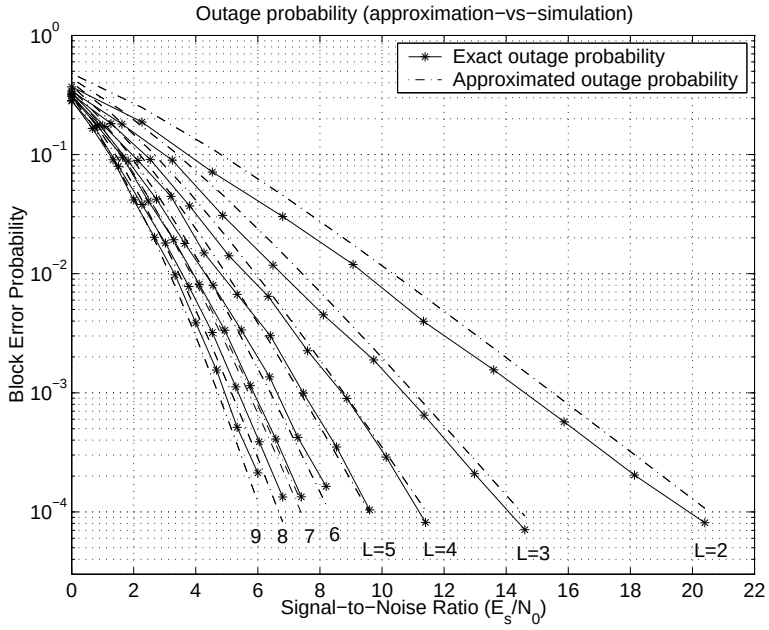

Fig. 6. Exact outage probability vs. the approximated outage probability for a coded OFDM system with $N = 1024$ subcarriers over a frequency-selective fading channel with $L = 2 \sim 9$ paths

Fig. 6 shows the exact outage probability as well as our approximated results for the coded OFDM system with $N = 1024$ subcarriers for various numbers of paths, $L = 2 \sim 9$. From that plot, we see that the exact outage probability is well approximated by (4.12), especially when the number of independent paths is large. This is expected because the approximation in (4.8) becomes more accurate when there are a large number of independent random variables.

3. Results of Practical Codes

In order to get an indication of how close we can get to the theoretical outage probability with practical codes, simulations are carried out using various coding schemes.

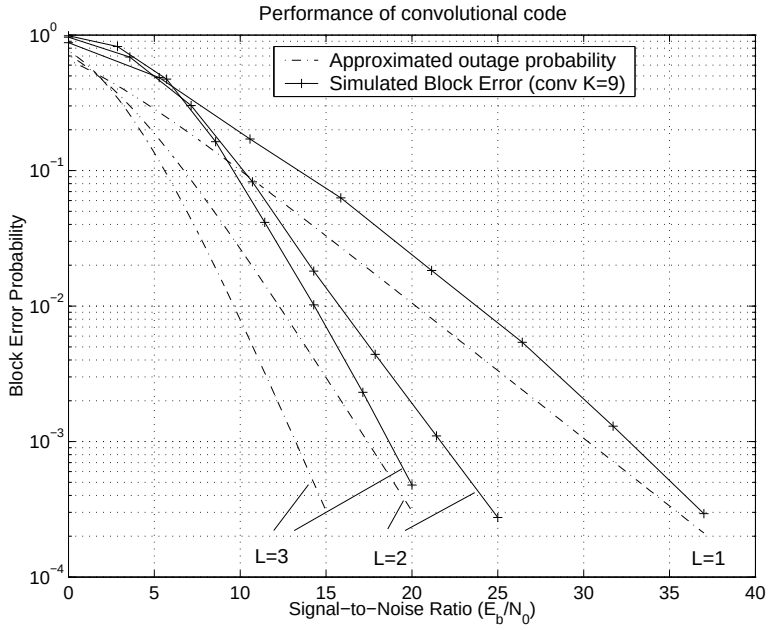

Fig. 7. Block error probability of a rate 1/2 terminated convolutional code with constraint length $K = 9$ and generator polynomial $(561, 753)$ compared with the approximated outage probability

In Fig. 7 and Fig. 8, the simulated block error probability of a rate 1/2 terminated convolutional code with constraint length $K = 9$ and generator polynomial $(561, 753)$ as well as a rate 1/2 turbo code with generator polynomial $(7, 5)$ are compared with the approximated outage probability for different numbers of paths $L = 1, 2, 3$. From the plots above, we can see that the optimum system performance can be achieved by some near Shannon capacity coding schemes, such as turbo code. This is a direct result of the information theoretical analysis approaches adopted in this thesis for the evaluation of the coded OFDM system performance.

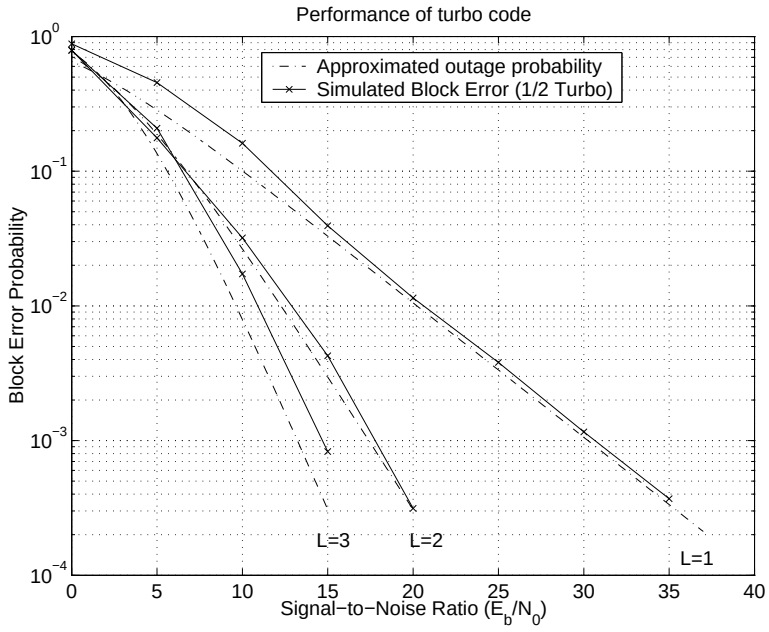

Fig. 8. Block error probability of a rate 1/2 turbo code with component generator polynomial $(7, 5)$ compared with the approximated outage probability

D. Conclusion on Performance Analysis

In this chapter, performance analysis of coded OFDM systems are investigated over frequency-selective fading channels. Both the random coding upper bounds and the strong converse lower bounds are derived and shown to converge to the channel outage probability for large OFDM block lengths. Hence the outage probability draws primary attention and is taken as the optimal performance indicator of a coded OFDM system. Instead of evaluating the outage probability numerically, an approximate but analytically close form expression of the outage probability is provided. Numerical results of the exact outage probability as well as the simulation results of a practical turbo-coded OFDM system well demonstrate and further confirms the fitness of this approximation.

Throughout the discussion in the chapter, we find this approximation of the outage probability not only provides us a guidance on evaluating various coding schemes for the coded OFDM system, but also serves as a handy tool to compare with other communication systems operating in the same multipath fading environment.

CHAPTER V

RATE AND POWER ALLOCATION OF CODED OFDM SYSTEMS

A. Assumption on Channel State Information

In this chapter, we assume there is a reverse link between the transmitter and receiver, which is not a stringent constraint in most wireless communication systems where communication is duplex and the channel stays comparably static between consecutive frames. Hence both the transmitter and receiver share the channel state information and adaptive rate and power allocation schemes at the transmitter are possible and expected to provide performance gain.

B. Adaptive-Modulation

When the channel experiences frequency-selective fading, the instantaneous signal to noise ratios $\gamma_i^{(t)}$ of the OFDM sub-carriers are different from each other. Thus it seems reasonable to apply large constellation sizes on sub-carriers of large SNRs, while applying small constellations or even stop transmitting information on sub-carriers which experience deep fading. Czylwik [12] proposes an adaptive modulation scheme for the individual sub-carriers in an OFDM system and the required signal to noise ratio for certain bit error probabilities is reduced dramatically compared with fixed modulations. Or equivalently, the maximum achievable information rate increases significantly under certain bit error probabilities with the same average power. However, due to the fact that channel capacity is an increasing function of the constellation size [20], the performance gain of adaptive modulation is obtained by increasing the constellation size and hence the channel capacity of sub-carriers with large SNRs. A fair comparison should be made between schemes of adaptive

modulation and schemes of fixed high order modulation with coding across the sub-carriers. This implies that instead of adapting the constellation size according to the SNRs of each sub-carrier, a good alternative is to implement the same high order modulation scheme among all sub-carriers, and adjust the information rate through coding in the frequency domain. Taken from an information theoretic point of view, the maximum achievable information rate $C_n(\boldsymbol{\alpha})$ is achieved by randomly generated codebooks given by (3.1) provided in Chapter III. Thus it is reasonable to believe that as far as the information rate is below the instantaneous channel capacity, the noise distorted symbols in small SNR sub-carriers can always be compensated by the high SNR symbols of other sub-carriers. And there is also great reduction in implementation complexity of this fixed modulation scheme since we don't have to change the constellation size and coding rate for each sub-carrier adaptively as well as transmit this information to the receiver correctly for successful decoding.

C. Power Allocation

It is well known that allocating the power over N independent parallel channels via water-filling can achieve maximum channel capacity. However, in this work we are interested in the capacity difference between water-filling and uniform power allocation. Through numerical evaluation, Czylwik [21] reported that we can only achieve a very small gain in throughput if the optimum power spectrum is used instead of a white power spectrum. In this paper, an analytical proof for this result is provided and the ultimate limit of this gain is established and demonstrated.

Proposition 1 *Assume we have a set of N AWGN channels in parallel. For channel i, the output y_i can be written as*

$$y_i = x_i + n_i \,, \tag{5.1}$$

with

$$n_i \sim \mathcal{N}_c(0, N_0), \tag{5.2}$$

and the complex noise n_i is assumed to be independent from channel to channel. The input has a power constraint on the total power used, such that

$$\frac{1}{2}E(|x_i|^2) = p_i \cdot |\alpha_i|^2 \cdot E_s, \qquad \sum_{i=1}^{N} p_i = N \ , \tag{5.3}$$

where the Rayleigh fading factor α_i has pdf given by (2.10) with variance $E[|\alpha_i|^2] = 1$, and fading is independent from channel to channel. The maximum average channel capacity C_{wf}^N is achieved by water-filling the power allocation,

$$C_{wf}^N = \max_{p_1,p_2,\cdots,p_N} \Big[\frac{1}{N}\sum_{i=1}^{N} C(\frac{p_i \cdot |\alpha_i|^2 \cdot E_s}{N_0})\Big] \ , \tag{5.4}$$

and the water-filling throughput is defined to be the ensemble average of this capacity over all possible fading realizations, which is given by

$$T_{wf}^N = E_{\alpha_1,\alpha_2,\cdots,\alpha_N}(C_{wf}^N)\,. \tag{5.5}$$

Then, for any integer N

$$T_{wf}^N \le T_{wf}^\infty \ . \tag{5.6}$$

Proof: Define region $\mathcal{U}$ to be

$$\mathcal{U} = \Big\{ p_1, p_2, \cdots, p_{2N} \Big| \sum_{i=1}^{N} p_i = N, \sum_{i=N+1}^{2N} p_i = N \Big\} \ . \tag{5.7}$$

According to the definition of C_{wf}^N in (5.4), we have the following inequality

$$\begin{aligned} T_{wf}^{2N} &\ge E_{\alpha_1,\alpha_2,\cdots,\alpha_{2N}}\Big(\max_{\mathcal{U}} \big(\frac{1}{2N}\sum_{i=1}^{2N} C(\frac{p_i \cdot |\alpha_i|^2 \cdot E_s}{N_0})\big)\Big) \\ &= E_{\alpha_1,\alpha_2,\cdots,\alpha_N}\Big(\max_{p_1,p_2,\cdots,p_N} \big(\frac{1}{2N}\sum_{i=1}^{N} C(\frac{p_i \cdot |\alpha_i|^2 \cdot E_s}{N_0})\big)\Big) \end{aligned}$$

$$+ E_{\alpha_{N+1},\alpha_{N+2},\cdots,\alpha_{2N}}\Big(\max_{p_{N+1},p_{N+2},\ldots,p_{2N}}\big(\frac{1}{2N}\sum_{i=N+1}^{2N} C(\frac{p_i\cdot|\alpha_i|^2\cdot E_s}{N_0})\big)\Big)$$
$$= \frac{1}{2}(T_{wf}^N + T_{wf}^N) = T_{wf}^N \ . \tag{5.8}$$

Thus, statement (5.6) is proved by the following sequence of inequalities

$$T_{wf}^N \le T_{wf}^{2N} \le T_{wf}^{4N} \le \cdots \le T_{wf}^{\infty} \ . \tag{5.9}$$

Proposition 2 *Assume we have the same set of N parallel channels described in Proposition 1. All conditions remain the same except that the fading factors α_i are assumed to be correlated to each other, rather than being independent fading factors between different parallel channels. The fading coefficients α_i, corresponding to the different OFDM sub-carriers, are related to fading envelopes c_i by*

$$\mathbf{c}^{N,L} = [c_1,\cdots,c_L,0,\cdots,0]^T \in \mathcal{C}^{N\times 1}, \tag{5.10}$$

$$\boldsymbol{\alpha}^N = [\alpha_1,\cdots,\alpha_N]^T \in \mathcal{C}^{N\times 1}, \tag{5.11}$$

$$\boldsymbol{\alpha}^N = W_{N\times N}\cdot\mathbf{c}^{N,L} \ , \tag{5.12}$$

where W is defined in (2.7). The fading envelope c_i for each path has a pdf given by (2.10) with variance $E[|c_i|^2] = 1/L$, and fading independently from path to path. With the same input power constraint and the same definition of water-filling channel capacity, the same inequality expressed in (5.6) holds.

Proof: Consider a set of $2N$ parallel channels with $2L$ independent fading paths. The fading envelope $\mathbf{c}^{2N,2L}$ can be represented as a combination of the two independent fading envelopes $\mathbf{c}_1^{N,L}$ and $\mathbf{c}_2^{N,L}$ by the following format

$$\mathbf{c}^{2N,2L} = [\,\mathbf{c}_1^{N,L^T},\,\mathbf{c}_2^{N,L^T}\,]^T \in \mathcal{C}^{2N\times 1} \ . \tag{5.13}$$

Using the following FFT property,

$$\begin{cases} \widehat{f}_{2k} &= \sum_{i=0}^{N-1} [f_i + f_{i+N}] \cdot w_N^{ik} \ , \\ \widehat{f}_{2k+1} &= \sum_{i=0}^{N-1} [(f_i - f_{i+N}) w_{2N}^{i}] \cdot w_N^{ik} \ , \end{cases} \tag{5.14}$$

we can rewrite $\boldsymbol{\alpha}$ as

$$\begin{cases} \alpha_{2k-1} = \sum_{i=1}^{N} d_{1_i} \cdot w_N^{(i-1)k} \ , \\ \alpha_{2k} \ \ = \sum_{i=1}^{N} d_{2_i} \cdot w_N^{(i-1)k} \ , \end{cases} \tag{5.15}$$

where

$$\begin{cases} d_{1_i} = c_{1_i} + c_{2_i} \ , \\ d_{2_i} = (c_{1_i} - c_{2_i}) \cdot w_{2N}^{(i-1)} \ . \end{cases} \tag{5.16}$$

It is obvious that d_{1_i} and d_{2_i} are independent Rayleigh fading sequences with equal variance $E[|d_{1_i}|^2] = E[|d_{2_i}|^2] = 1/L$. Thus, region $\mathcal{U}$ is defined to be

$$\mathcal{U} = \Big\{ p_1, p_2, \cdots, p_{2N} \Big| \sum_{i=1}^{N} p_{2i} = N, \sum_{i=1}^{N} p_{2i-1} = N \Big\}, \tag{5.17}$$

and an inequality similar to (5.8) is obtained,

$$\begin{aligned} T_{wf}^{2N,2L} &\geq E_{\alpha_1,\alpha_2,\cdots,\alpha_{2N}} \Big(\max_{\mathcal{U}} \Big(\frac{1}{2N} \sum_{i=1}^{2N} C(\frac{p_i \cdot |\alpha_i|^2 \cdot E_s}{N_0}) \Big) \Big) \\ &= E_{\alpha_1,\alpha_3,\cdots,\alpha_{2N-1}} \Big(\max_{p_1,p_3,\ldots,p_{2N-1}} \Big(\frac{1}{2N} \sum_{i=1}^{N} C(\frac{p_{2i-1} \cdot |\alpha_{2i-1}|^2 \cdot E_s}{N_0}) \Big) \Big) \\ &+ E_{\alpha_2,\alpha_4,\cdots,\alpha_{2N}} \Big(\max_{p_2,p_4,\ldots,p_{2N}} \Big(\frac{1}{2N} \sum_{i=1}^{N} C(\frac{p_{2i} \cdot |\alpha_{2i}|^2 \cdot E_s}{N_0}) \Big) \Big) \\ &= \frac{1}{2}(T_{wf}^{N,L} + T_{wf}^{N,L}) = T_{wf}^{N,L} \ . \end{aligned} \tag{5.18}$$

Finally the statement proves that

$$T_{wf}^{N,L} \leq T_{wf}^{2N,2L} \leq \cdots \leq T_{wf}^{\infty,\infty} \ . \tag{5.19}$$

Through Propositions 1 and 2, the ultimate limit of water-filling throughput is known to be T_{wf}^{∞} and $T_{wf}^{\infty,\infty}$, where there are infinite number of independent fading

variables in both cases. According to the law of large numbers, the sample distribution of $|\alpha_i|$ converges to the ensemble Rayleigh distribution with probability 1. This means that the relative proportion of occurrences of the fading factor $|\alpha_i|$ is proportional to its ensemble distribution, and can be expressed by the following form

$$\lim_{N\to\infty} \frac{\left|\left\{\alpha_i \;\middle|\; |\alpha_i| \in [x-\varepsilon/2, x+\varepsilon/2]\right\}\right|}{N\cdot\varepsilon} = f(x), \tag{5.20}$$

where $f(\cdot)$ is given by (2.10). Thus the problem is reduced to a standard constrained optimization problem. Applying the Kuhn-Tucker condition and after tedious but straightforward calculus, the solution for the above two cases are obtained.

When the input symbol x_i has an unconstrained alphabet and the receiver performs soft decisions, the water-filling throughput over the ensemble fading realizations is given by

$$T_{wf}^{\infty} = \int_0^{\infty} \log_2(\,1+p(|\alpha|)\cdot|\alpha|^2\cdot\gamma_s\,)\cdot f(|\alpha|)\cdot d\,|\alpha| = \left[\mu\cdot\exp(-\frac{1}{\mu\cdot\gamma_s})-1\right]\cdot\gamma_s \;, \tag{5.21}$$

where $f(\cdot)$ is given by (2.10),

$$\gamma_s = \frac{E_s}{N_0}\;, \tag{5.22}$$

and

$$p(|\alpha|) = (\mu - \frac{1}{|\alpha|^2\gamma_s})^+, \tag{5.23}$$

where μ is chosen such that

$$\int_0^{\infty} p(|\alpha|)\cdot f(|\alpha|)\cdot d\,|\alpha| = 1. \tag{5.24}$$

Here $(x)^+$ denotes the positive part of x, i.e.,

$$(x)^+ = \begin{cases} x \text{ if } x \geq 0, \\ 0 \text{ if } x < 0. \end{cases} \tag{5.25}$$

When BPSK modulation with soft decisions is used as the channel model, and approximation (3.15) is taken to be the conditional sub-channel capacity, the throughput can be written as

$$T_{wf}^{\infty} = 1 - \int_0^{\infty} \exp(\, -m \cdot p(|\alpha|) \cdot \gamma_s \,) \cdot f(|\alpha|) \cdot d\,|\alpha| \ , \tag{5.26}$$

where $f(\cdot)$ is given by (2.10), γ_s is given by (5.22), and

$$p(|\alpha|) = \Big(\frac{\log(m\gamma_s) - \mu}{m\gamma_s} \Big)^{+}, \tag{5.27}$$

where μ is chosen to satisfy (5.24).

Taken as the reference system, the throughput of uniform power allocation among the OFDM sub-carriers averaged over the ensemble of fading realizations is given by

$$T_{up} = \int_0^{\infty} C(|\alpha|^2\gamma_s) \cdot f(|\alpha|) \cdot d\,|\alpha| \ . \tag{5.28}$$

Plugging (3.13) and (3.15) into the above definition, we get

$$T_{up} = \begin{cases} -E_i(-\frac{1}{\gamma_s}) \cdot \exp(\frac{1}{\gamma_s}), & \text{for unconstrained input alphabets} \ , \\ \frac{m\cdot\gamma_s}{1+m\cdot\gamma_s}, & \text{for binary input alphabets} \ , \end{cases} \tag{5.29}$$

where $m = 1.24$ and the exponential integral function is given by

$$E_i(x) = e_0 + \log(-x) + \sum_{k=1}^{\infty} \frac{x^{-k}}{k \cdot k!}, \quad e_0 \simeq 0.5772 \quad . \tag{5.30}$$

Using the results given by (5.21), (5.26), and (5.29) , $\eta(\gamma_s)$ is further defined to be the ultimate throughput gain of the water-filling power allocation with infinite number of independent fading variables versus the uniform power allocation,

$$\eta(\gamma_s) = \frac{T_{wf}^{\infty} - T_{up}}{T_{wf}^{\infty}} \quad . \tag{5.31}$$

In Fig. 9, numerical results of the water-filling throughput T_{wf}^{N} and $T_{wf}^{N,L}$, as well as the ultimate limit T_{wf}^{∞} are compared with the throughput T_{up} of uniform power allocations for the channels with unconstrained input alphabets. We have evaluated the water-filling throughput for different numbers of independent parallel channels with $N = 2, 16, 128$, as well as the throughput for correlated channels, which are the sub-carriers of the OFDM system with frame length 1024 and independent multi-path numbers, $L = 2, 16, 128$. For illustration purposes, Fig. 9 includes only the cases of $N = 2, 16$ for independent channels and $L = 2, 16$ for correlated channels, since the throughput curves are getting very close to the ultimate throughput curve T_{wf}^{∞} when $N \geq 16$ ($orL \geq 16$). The ultimate throughput gain of the water-filling power allocation versus the uniform power allocation, given by (5.31), is illustrated in Fig. 10. Similar results of throughput and throughput gain for the channels with a binary input alphabet and soft outputs are shown in Fig. 11 and Fig. 12.

From the results in Fig. 9-12, it is seen that for both the unconstrained input alphabet or the binary input alphabet, water-filling the power among different parallel channels adaptively only achieves a limited gain in terms of throughput. The ultimate gain plotted in Fig. 12 further demonstrates that for the binary input channel the additional throughput achieved by water-filling in an OFDM system is less than 5% as long as the average signal-to-noise-ratio is larger than $2dB$. This implies that with high probability, the capacity gain compared with uniform power allocation is insignificant, although water-filling is optimal at any given channel realization. Thus, an insignificant amount of average channel capacity is lost in the long run when using uniform power allocation instead of performing power allocation adaptively according to the instantaneous signal to noise ratio of each sub-carrier.

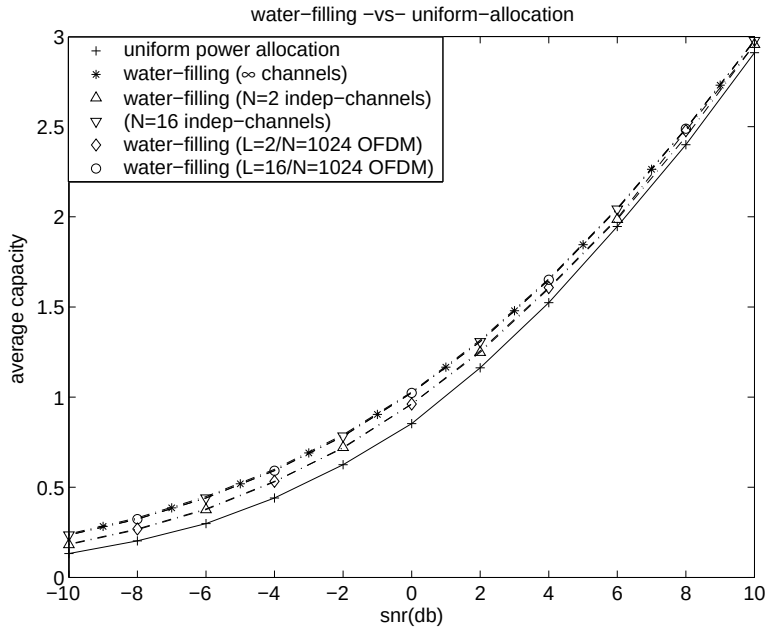

Fig. 9. Throughput comparison between the water-filling power allocation and the uniform power allocation (for unconstrained input and soft output channels)

D. Rate Allocation

In Section C, we reached the conclusion that from an information-theoretic standpoint water-filling is not a promising technique for coded OFDM systems over a fading environment. However, the discussion is based upon the assumption that the information rate of the OFDM system is adjusted adaptively according to the instantaneous channel state information. This implies that the system always transmits with the maximum information rate that the channel can support at any given time. This adaptive nature is reasonable when the channel changes slowly and is thus easy to track. However, a potential problem is incurred when the channel is rapidly changing or when the application cannot afford timely and accurate feedback. Under this situation, the information rate must be fixed during the entire fading process.

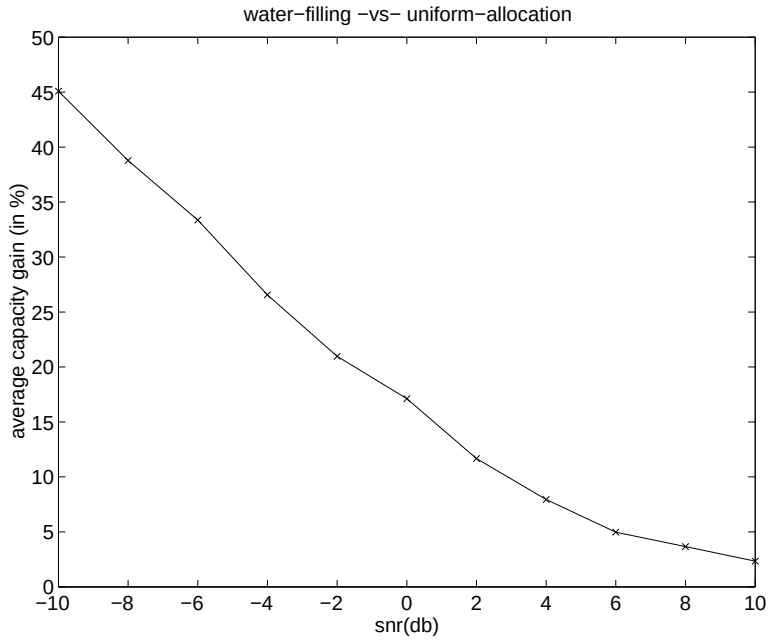

Fig. 10. Ultimate throughput gain of the water-filling power allocation over the uniform power allocation (for unconstrained input and soft output channels)

Suppose the instantaneous channel capacity $C_n(\mathbf{c})$ has a distribution $g_{C_n}(x)$ illustrated in Fig. 13. Define T_a and T_f to be the throughput (average information rate over the ensemble fading realizations $\mathbf{c}$) of the rate-adaptive and rate-fixed schemes respectively, given by the following equations

$$T_a = E_{\mathbf{c}}\Big[\, C_n(\mathbf{c}) \,\Big] = \int_0^\infty x \cdot g_{C_n}(x)\, d\, x \ \ , \tag{5.32}$$

$$T_f = \max_{R_f} \left(\, R_f \cdot P_r\Big(C_n(\mathbf{c}) \geq R_f\Big) \, \right) = \max_{R_f} \Big(R_f \cdot \int_{R_f}^\infty g_{C_n}(x)\, d\, x \Big) \ . \tag{5.33}$$

It is quite clear from (3.10), (3.12), (3.13), and (3.14) that the instantaneous channel capacity $C_n(\mathbf{c})$ is a highly nonlinear function of the vector $\mathbf{c}$. Generally speaking, it is very difficult if not impossible to get the pdf (or cdf) of a random vector's non-linear transformation. By applying the central limit theorem to $C_n(\mathbf{c})$

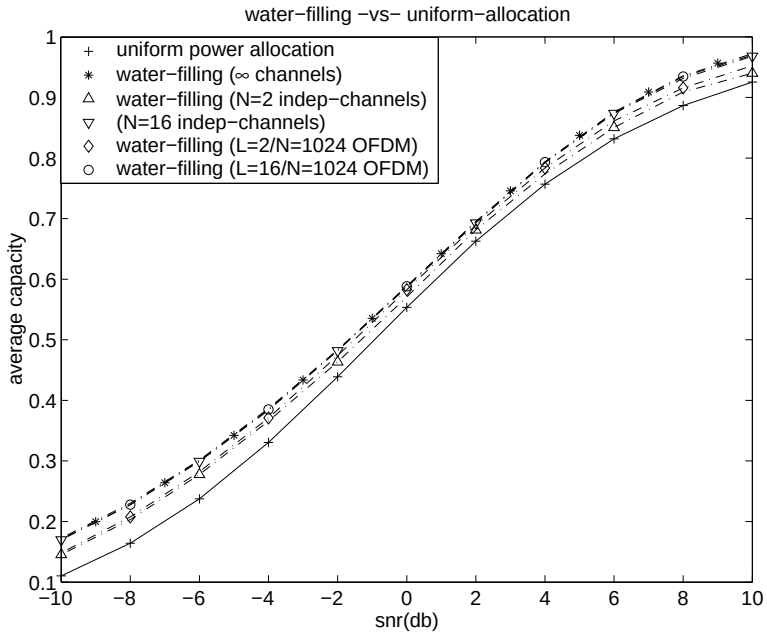

Fig. 11. Throughput comparison between the water-filling power allocation and the uniform power allocation (for binary input and soft output channels)

when there are a large number of independent paths, its pdf is well approximated by a Gaussian distribution for the range in which we are interested.

In order to illustrate the fitness of this approximation, the histograms of the instantaneous channel capacity $C_N(\boldsymbol{\alpha}^{(t)})$ for the OFDM system with 1024 sub-carriers are shown in Fig. 14. For a common signal to noise ratio ($\gamma_s = 4dB$), each solid curve in the above plot represents a histogram with a different number of paths ($L = 2, 5, 10, 40, 100$ respectively). Their corresponding Gaussian approximations are also shown as the dotted curves for comparison. Note that this approximation may become nonsense in certain capacity ranges, such as $C_N \leq 0$, for the capacity is a non-negative variable. Fortunately, we are not interested in the tail part of this distribution, which only corresponds to an insignificant amount of throughput. From this point of view, it is seen that the instantaneous channel capacity is well

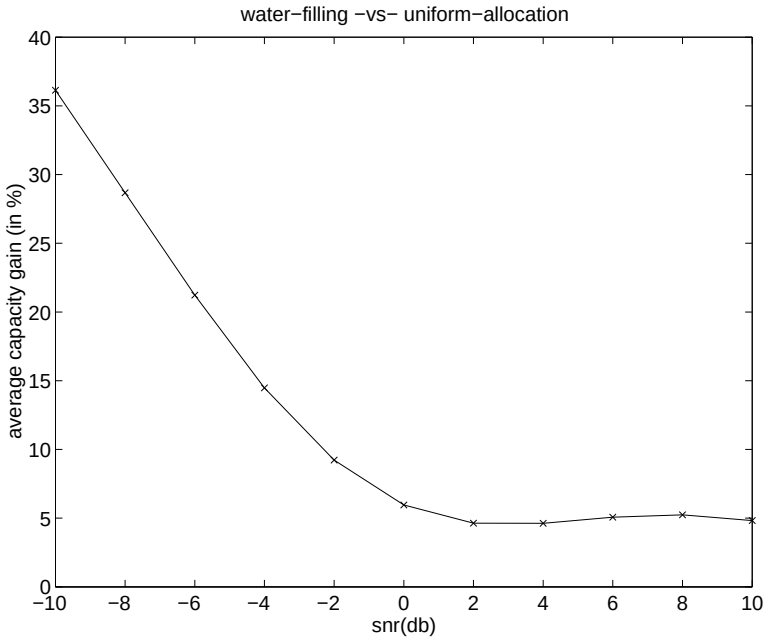

Fig. 12. Ultimate throughput gain of the water-filling power allocation over the uniform power allocation (for binary input and soft output channels)

approximated as a Gaussian random variable when the multi-path fading spreads over more than 5 taps, which is a reasonable assumption in many applications.

For the sake of simplicity, the following discussion focuses on binary input symbols, since it is straightforward to extend the results to larger alphabets. According to (3.15) and (2.6), the following mean and variance for $C_N(\mathbf{c}^{(t)})$ are obtained:

$$E[\, C_N(\mathbf{c}^{(t)})\,] = \frac{m\gamma_s}{1+m\gamma_s}\,, \tag{5.34}$$

$$Var[\, C_N(\mathbf{c}^{(t)})\,] = \frac{1}{N}\sum_{k=0}^{N-1} \frac{1}{(1+m\gamma_s)^2 - (m\gamma_s)^2\cdot|r_k|^2} \;-\; \frac{1}{(1+m\gamma_s)^2}\,, \tag{5.35}$$

where

$$r_k = \frac{1}{L}\cdot\frac{\sin\left(kL\pi/N\right)}{\sin\left(k\pi/N\right)}\,, \tag{5.36}$$

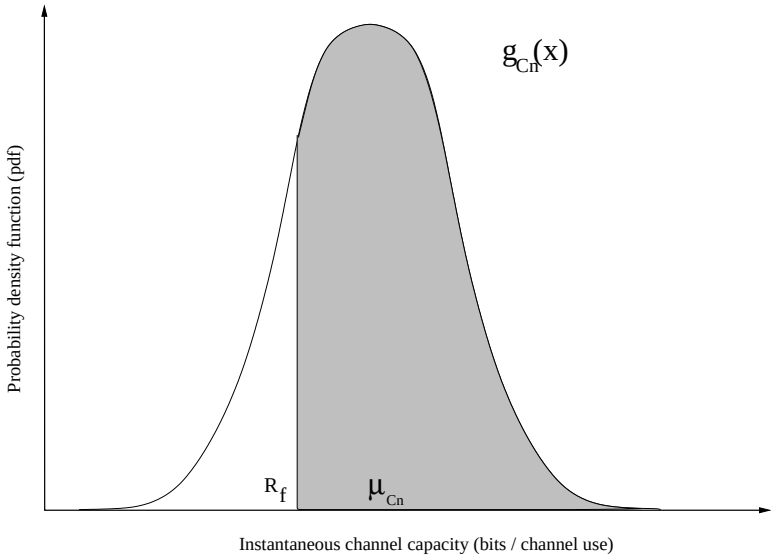

Fig. 13. PDF of the instantaneous channel capacity

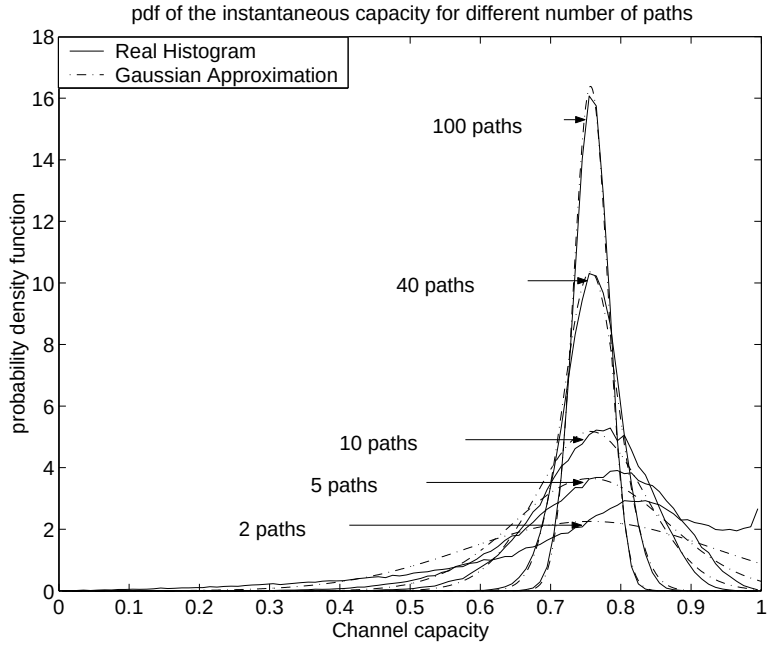

Fig. 14. Histogram of the instantaneous channel capacity for an OFDM system with 1024 sub-carriers, and $L = 2, 5, 10, 40, 100$ independent fading paths

and

$$m = 1.24, \qquad \gamma_s = \frac{E_s}{N_0}\,. \tag{5.37}$$

Recall that N is the number of sub-carriers in one OFDM frame and L represents the number of independent paths in the frequency-selective fading channels. When $L \ll N$, which is a reasonable assumption for OFDM systems, (5.35) can further be simplified and approximated by

$$Var[\,C_N(\mathbf{c}^{(t)})\,] = \sum_{k=1}^{\infty} \frac{(m\gamma_s)^{2k}}{(1+m\gamma_s)^{2k+2}} \cdot h_k(L) \approx \sum_{k=1}^{K} \frac{(m\gamma_s)^{2k}}{(1+m\gamma_s)^{2k+2}} \cdot h_k(L)\,, \tag{5.38}$$

where the approximation is carried out by taking into account only the first K terms of the series. The variance of the instantaneous channel capacity is well approximated by the truncated series of truncation length $K = 5$ in a wide SNR range. The first five terms of $h_k(L)$ are given by

$$\begin{aligned}
h_1(L) &= 1,\\
h_2(L) &= (1+2L^2)L^2/3,\\
h_3(L) &= (4+5L^2+11L^4)L^4/20,\\
h_4(L) &= (45+49L^2+70L^4+151L^6)L^6/315,\\
h_5(L) &= (4032+4100L^2+5187L^4+7350L^6)+15619L^8)L^8/36288\,.
\end{aligned} \tag{5.39}$$

A detailed derivation of the approximation process is given in Appendix B.

Suppose it takes up to l OFDM frames to form one codeword. In quasi-static fading channels, where the fading envelope $\mathbf{c}^{(t)}$ is assumed to be constant during one codeword, but independent from codeword to codeword, the mean and variance of the instantaneous channel capacity are

$$\mu_{C_n} = E[\,C_n(\mathbf{c})\,] = \frac{1}{l}\sum_{t=1}^{l} E[\,C_N(\mathbf{c}^{(t)})\,] = E[\,C_N(\mathbf{c}^{(t)})\,] = \mu_{C_N}, \tag{5.40}$$

$$\sigma^2_{C_n} = Var[\, C_n(\mathbf{c})\,] = Var\Big[\, \frac{1}{l}\sum_{t=1}^{l} C_N(\mathbf{c}^{(t)})\,\Big] = Var[\, C_N(\mathbf{c}^{(t)})\,] = \sigma^2_{C_N}. \tag{5.41}$$

In fast fading channels, where $\mathbf{c}^{(t)}$ is independent from time to time, the mean and variance are

$$\mu_{C_n} = E[\, C_N(\mathbf{c}^{(t)})\,] = \mu_{C_N}, \tag{5.42}$$

$$\sigma^2_{C_n} = \frac{1}{l} Var[\, C_N(\mathbf{c}^{(t)})\,] = \frac{1}{l}\sigma^2_{C_N}. \tag{5.43}$$

Applying a Gaussian approximation to (5.32) and (5.33), T_a and T_f can be written as

$$T_a = \mu_{C_n}, \tag{5.44}$$

$$T_f = \max_{R_f}\Big[\; R_f \cdot Q(\frac{\mu_{C_n} - R_f}{\sigma_{C_n}})\;\Big]. \tag{5.45}$$

From (5.38), it is seen that by increasing the number of independent paths L or the signal to noise ratio γ_s, the variance of the instantaneous channel capacity will decrease. It is also known that the throughput loss of the fixed-rate scheme is due to the following two reasons: 1) the code rate is fixed at R_f even when the channel can support higher information rates; and 2) once the instantaneous channel capacity falls below R_f, the achievable information rate decreases to zero. Thus when the channel has a large number of independent paths or a high signal to noise ratio, the small capacity variance will cause the pdf $g_{C_n}(x)$ to become spike-shape. It is then obvious from Fig. 13 that the throughput difference between T_a and T_f will be diminished making rate-adaptation less important.

Taking the throughput T_a of the adaptive-rate schemes as a reference, which is normalized to be 1, the throughput of the fixed-rate schemes for different number of paths and different signal to noise ratios is shown in Fig. 15. In the top sub-plot, each curve represents the throughput of the OFDM system with 1024 sub-carriers and L paths. From the bottom to the top, the number of paths increases

as $L = 1, 2, 5, 10, 40, 100$. The bottom sub-plot illustrates the corresponding optimal rate needed to achieve these throughputs. Notice that the underlying assumption for the throughput obtained in this section is that the ideal Shannon code is available at any given rate.

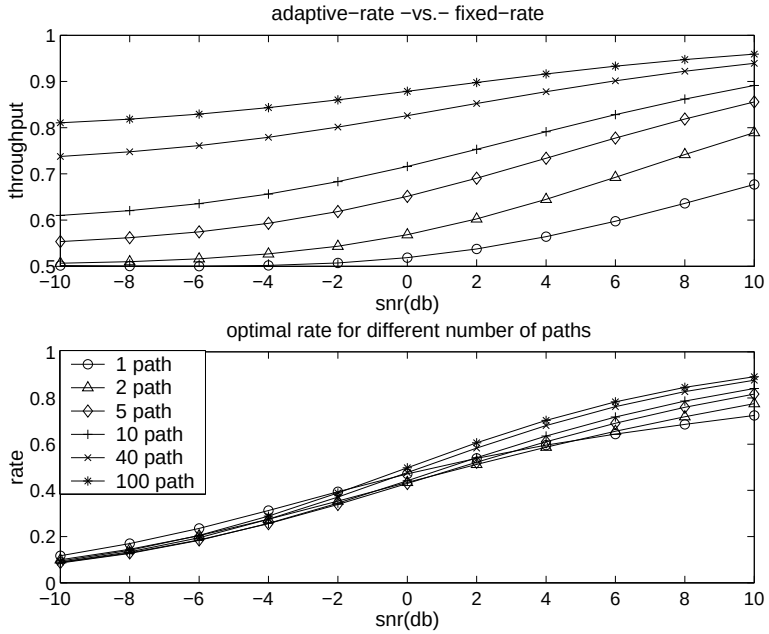

Fig. 15. Ideal throughput comparison between the rate-adaptive schemes and the rate-fixed schemes (under the condition of perfect coding and infinite available code rates)

From the plot, it is seen that the throughput increases with the average signal to noise ratio γ_s and the number of independent paths L, which is consistent with the analysis in equation (5.38). Taken from another point of view, increasing the system power will cause the system to operate in a capacity region near 1 with high probability and hence adjusting the information rate adaptively is less important. Increasing the system diversity order has an effect of averaging the system performance, which means that the probability of all channels running into extremely good

or bad situations decreases, making adapting the rate have a less significant impact on the system throughput. Further more, it is seen from Fig. 15 that the throughput of the fixed-rate schemes achieves more than 75% of the throughput of adaptive-rate schemes, when there are at least 5 paths with total signal to noise ratio greater than $4dB$.

E. Practical Schemes

So far, our discussion is based upon the analysis of the ideal information rate and throughput. To complement the theoretical results, two practical coded OFDM systems are introduced to implement an adaptive-rate and a fixed-rate scheme as discussed above.

In order to implement adaptive schemes, both the transmitter and the receiver are required to have knowledge of the channel state information. Notice that all of the information about the channel state at the transmitter is obtained from the receiver through a feedback link. Adaptive schemes which require immediate CSI feedback for the transmitter to decide appropriate transmission rates would probably be impractical, especially in a fast fading environment. Thus a rate compatible punctured turbo code combined with an automatic repeat-request protocol (RCPT-ARQ) [22], which only requires a simple low rate feedback channel without any delay requirement, and takes advantage of the powerful turbo code, has been implemented in our application.

The binary source is first encoded into blocks in accordance with a low redundancy (n, k) block error detection code. This encoded data source is input to the RCPT encoder which turbo encodes the data sequence and partitions the resulting code symbols of each systematic and parity stream into sub-blocks of size $(n/p = N)$, where p is called the puncturing period. The underlying rate $1/M$ turbo encoder, con-

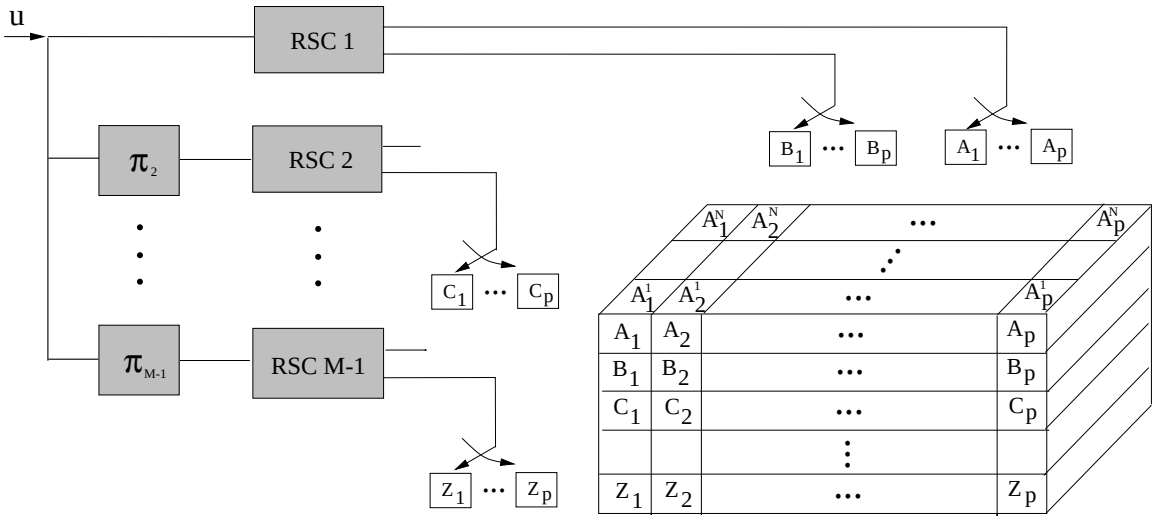

Fig. 16. Rate compatible punctured turbo (RCPT) encoder

sists of $M-1$ rate $1/2$ constituent recursive systematic convolutional (RSC) encoders. Note that the composite encoders can have other rates, and need not necessarily be equal rate. As shown in Fig. 16, the systematic bits of all but the first encoder are discarded and the resulting single systematic plus (M-1) parity streams are arranged into a block structure shown in the figure, which partitions each stream into p sub-blocks. The sub-block A_1, for example, contains a fraction $1/P$ of the systematic bits consisting of bit 0, bit p, bit $2p$, etc. If we take each of these sub-block as an element of an $M \times p$ matrix, as shown in the figure, each row corresponds to a different systematic/parity stream, and each column refers to a different decimated subsequence of that data stream. The interleavers, $\{\pi_i\}_{i=2}^{M-1}$ are "S-random" permutations [23], which satisfy a distance condition ensuring that each symbol to be permuted is a distance S or more from the previous S adjacent symbols.

According to the RCPT puncturing rule, each codeword consists of one or more sub-blocks of the above turbo encoded data such that at least $p+1$ sub-blocks are

sent, and no sub-block is sent twice. This code construction allows for a family of codes rates

$$R_r = \frac{p}{p+r}, \quad 1 \leq r \leq (M-1)p \ . \tag{5.46}$$

A binary $M \times p$ puncturing matrix $\mathbf{a}(r)$ is associated with each rate R_r in a manner that the ones in the matrix $\mathbf{a}(r)$ of a higher rate code must be covered by the puncturing matrix of any lower rate code. By overlaying the matrix $\mathbf{a}(r)$ over the depicted matrix of data as shown Fig. 16, the RCPT codeword of rate R_r can be constructed by selecting the sub-blocks of data corresponding to each 1 in the puncturing matrix and sending them over N sub-carriers as one OFDM frame.

For the sake of simplicity, we assume, without loss of generality, a selective-repeat ARQ strategy is implemented, noting that the RCPT-ARQ protocol can be trivially adapted to either stop-and-wait or go-back-N schemes. It is further assumed that a low rate error-less feedback channel is available from the receiver to transmitter which guarantees one bit acknowledge information received by the transmitter correctly from the receiver once every OFDM frame.

The RCPT-ARQ protocol performs the following steps:

1. Encode k information bits by a (n, k) block error detection code. Input the n bit coded bits into the rate $1/M$ RCPT encoder. Store the resulting M systematic and parity streams at the transmitter, for potential transmission.

2. Initialize $r = 1$.

3. Transmit the sub-blocks as indicated by $\mathbf{a}(r)$ (that have not yet been transmitted)

4. Decode the rate R_r RCPT code using the code symbols received so far. After each iterative decoding process, hard quantize the likelihood ratios on the

systematic sequence and calculate the syndrome of the (n, k) error detection codeword. Exit the iterative loop, output the k decoded information bits and send an ACK to the transmitter, when there is an all-zeros syndrome. Otherwise, continue the iterative decoding process until a maximum number of iterations and send a NAK to the transmitter if the syndrome is still nonzero.

5. At the transmitter, reset the protocol and proceed to step 1) if an ACK is received, or increment r to the next available value and proceed to step 3) when a NAK is received.

Notice that instead of giving up and reseting the protocol when the decoding fails after the transmission of all the systematic and parity symbols $[r = (M-1)p]$, as in the above schemes, alternative schemes such as packet combining [24] and data merging [25] strategies can provide better performance. Detailed comparison of these schemes is beyond the scope of this thesis.

The above RCPT-ARQ schemes fall into the so-called class of redundancy incremental Hybrid-ARQ protocols in the sense that the parity information is incrementally transmitted to adaptively meet the error performance requirement of the the system. This is also appealing from an information theoretic standpoint that no received information is discarded (as is the case of other Hybrid-ARQ schemes). However by performing redundancy-combing in the above RCPT-ARQ schemes, we are paying almost $\overline{l} - p$ times decoding complexity than the regular turbo code with the same codeword length, where $\overline{l}$ is the average number of transmitted sub-blocks that result in a successful decoding. Thus the simple Hybrid-ARQ scheme combined with a fixed rate RCPT code would be good candidate when the application cannot afford the complexity required by RCPT-ARQ, or when the throughput difference between these two schemes is not that significant.

F. Throughput Analysis of Practical Schemes

Generally, throughput and accepted packet error rate are the two parameters that are of most interests to us. In this section, the analysis of these two parameters is provided for the previously described ARQ schemes.

The decoded information bits from the turbo decoder are not independent since the decoder makes decisions based on the whole received sequence and hence the decoded bits are correlated. However, due to the fact that the component convolutional codes have a short memory, usually of only 4 bits or less, the correlation of the output information sequence only exists between a few neighboring bits. Being randomly deinterleaved as opposed to the interleaver between the outer error detection code and inner RCPT code, the correlation has been scrambled and averaged over the whole sequence. Hence the correlation between the output bits is fairly small and it is reasonable to assume an $i.i.d$ decoded information sequence from the turbo decoder with bit error probability p_b. The accepted packet error probability is then given by

$$P_a(E) = \sum_{j=d_{min}}^{n} A_j \cdot p_b^j (1-p_b)^{n-j} \quad , \tag{5.47}$$

where A_j is the weight distribution of the (n, k) block code. Although the weight distribution of an extended BCH code, which is used as the error detection code, is known in most cases, the error performance of the turbo code itself is a challenging problem. Thus we resort to a simple upper bound as shown below

$$P_a(E) \leq \sum_{j=d_{min}}^{n} A_j \cdot p_b^j (1-p_b)^{n-j} \Big|_{p_b=\frac{1}{2}} = 2^{-(n-k)} \quad . \tag{5.48}$$

For example, the accepted packet error rate $P_a(E)$ for a $(1024, 993)$ extended BCH code with $d_{min} = 8$ is less than 4.7×10^{-10}. The numerical results in the next section will further verify this result.

The analytical results obtained in Section D are for an ideal Shannon code with arbitrary code rates available at the transmitter. Due to the imperfection of the turbo code, and finite puncturing period p, there is a limited number of available code rates, and hence the system performance in terms of throughput will degrade somewhat. For the sake of discussion, the critical capacity for a given RCPT code with rate R_r is defined to be $C_{th}^{R_r}$, such that the probability of decoding error is assumed to be zero when the instantaneous channel capacity is beyond this threshold, and on the other hand, the error probability is regarded as one when the instantaneous channel capacity falls below this value. Thus the throughput for Hybrid-ARQ and redundancy incremental Hybrid-ARQ schemes in a quasi-static fading channel is given by

$$T_a = \frac{p \cdot (1 - q_{_{(M-1)p+1}})}{\sum_{r=1}^{(M-1)p}(p+r) \cdot q_r + Mp \cdot q_{_{(M-1)p+1}}} \ , \tag{5.49}$$

$$T_f = \max_r \Big(\frac{p}{p+r} \cdot s_r\Big) \ . \tag{5.50}$$

Where each q_r and s_r represent probabilities such that

$$q_1 = P_r\Big(C_{th}^{R_1} \le C_N(\mathbf{c})\Big) = Q\Big(\ \frac{C_{th}^{R_1} - \mu_{_{C_N}}}{\sigma^2_{_{C_N}}}\ \Big), \tag{5.51}$$

$$\begin{aligned} q_{r+1} &= P_r\Big(C_{th}^{R_{r+1}} \le C_N(\mathbf{c}) \le C_{th}^{R_r}\Big) \\ &= Q\Big(\frac{C_{th}^{R_{r+1}} - \mu_{_{C_N}}}{\sigma^2_{_{C_N}}}\ \Big) - Q\Big(\frac{C_{th}^{R_r} - \mu_{_{C_N}}}{\sigma^2_{_{C_N}}}\Big), 1 \le r \le (M-1)p - 1, \end{aligned} \tag{5.52}$$

$$q_{(M-1)p+1} = P_r\Big(C_N(\mathbf{c}) \le C_{th}^{R_{(M-1)p}}\Big) = 1 - Q\Big(\ \frac{C_{th}^{R_{(M-1)p}} - \mu_{_{C_N}}}{\sigma^2_{_{C_N}}}\ \Big), \tag{5.53}$$

and

$$s_r = P_r\Big(C_{th}^{R_r} \le C_N(\mathbf{c})\Big) = Q\Big(\ \frac{C_{th}^{R_r} - \mu_{_{C_N}}}{\sigma^2_{_{C_N}}}\ \Big), \quad 1 \le r \le (M-1)p\,. \tag{5.54}$$

For fast fading channels, T_a and T_f are given by the same equations, (5.49) and (5.50),

while q_r and s_r are given by

$$q_1 = P_r\Big(C_{th}^{R_1} \le \frac{1}{p+1}\sum_{t=1}^{p+1} C_N(\mathbf{c}^{(t)})\Big) = Q\Big(\frac{C_{th}^{R_1} - \mu_{C_N}}{\sigma_{C_N}^2/(p+1)}\Big), \tag{5.55}$$

$$\begin{aligned} q_{r+1} &= P_r\Big(C_{th}^{R_{r+1}} \le \frac{1}{p+r+1}\sum_{t=1}^{p+r+1} C_N(\mathbf{c}^{(t)}) \bigcap C_{th}^{R_r} \ge \frac{1}{p+r}\sum_{t=1}^{p+r} C_N(\mathbf{c}^{(t)})\Big) \\ &= \int_{-\infty}^{(p+r)C_{th}^{R_r}} \frac{1}{\sqrt{2\pi}} \exp\Big(-\frac{(x-(p+r)\mu_{C_N})^2}{(p+r)\sigma_{C_N}^2}\Big) \\ &\quad \cdot Q\Big(\frac{(p+r+1)C_{th}^{R_{r+1}} - x - \mu_{C_N}}{\sigma_{C_N}^2}\Big)\, dx, \quad 1 \le r \le (M-1)p-1, \end{aligned} \tag{5.56}$$

$$q_{(M-1)p+1} = P_r\Big(\frac{1}{Mp}\sum_{t=1}^{Mp} C_N(\mathbf{c}^{(t)}) \le C_{th}^{R_{(M-1)p}}\Big) = 1 - Q\Big(\frac{C_{th}^{R_{(M-1)p}} - \mu_{C_N}}{\sigma_{C_N}^2/Mp}\Big), \tag{5.57}$$

and

$$s_r = P_r\Big(C_{th}^{R_r} \le \frac{1}{p+r}\sum_{t=1}^{p+r} C_N(\mathbf{c}^{(t)})\Big) = Q\Big(\frac{C_{th}^{R_r} - \mu_{C_N}}{\sigma_{C_N}^2/(p+r)}\Big), \quad 1 \le r \le (M-1)p\,. \tag{5.58}$$

Since the regular performance bounds for turbo codes [26], or the density evolution method introduced in [27] [28], only provide reasonable results for asymptotic analysis (as block size goes to infinity) and assumes a perfect interleaver structure, we thus resort to the simulations, and represent the critical capacity $C_{th}^{R_r}$ as

$$C_{th}^{R_r} = 1 - \exp(-m \cdot \gamma_{th}^{R_r})\ , \tag{5.59}$$

where $\gamma_{th}^{R_r}$ is the simulated signal to noise ratio required to achieve the critical bit error probability p_{th} for a given RCPT code with rate R_r in an AWGN channel. Notice that the critical capacity obtained here is from simulation results in an AWGN channel, not the fading environment, but it gives us a crude indication of correct decoding when comparing the instantaneous channel capacity with this threshold. The numerical results in Section G will illustrate the usefulness of this analysis and shed some insights into the system design.

G. Simulation Results

Simulations were conducted to estimate the throughput of the proposed Hybrid-ARQ and redundancy incremental Hybrid-ARQ coded OFDM systems, and to compare these results with the analytical throughput obtained in Section C and D.

For the RCPT-ARQ schemes, the underlying turbo encoder consists of two rate 1/2 RSC encoders with generator polynomial $(1, 21/37)_{octal}$. The S-random interleavers used in the simulations were selected via an *ad hoc* search procedure [29]. The puncturing period p is 4 and all possible RCPT code rates were used. The optimal puncturing table, given by Table I, is chosen according to [22] via computer search. The log-MAP algorithm was used for the SISO decoding element and the maximum number of iterations allowed at any given decoding attempt was fixed at 8. In the simulations, the ARQ protocol terminated upon reaching the lowest code rate $(1/M)$ and the received codeword of that unsuccessful block is simply discarded. For the results presented in this section, an OFDM system with $N = 256$ sub-carriers is employed as the simulation model. The information block size of the turbo code is $n = pN = 1024$. A triple-error-correcting systematic extended binary primitive BCH code (1024,993) is implemented as the low redundancy error detection code. For the simple Hybrid-ARQ schemes, a fixed rate RCPT code is used for a given signal to noise ratio γ_s and a given number of paths L in the same OFDM system with 256 sub-carriers.

The simulated throughput for the Hybrid-ARQ and redundancy incremental Hybrid-ARQ under both quasi-static fading and fast fading environments are shown in Fig. 17. The ideal throughput of the adaptive-rate and fixed-rate schemes under these two fading conditions are also illustrated for comparison. For illustration purposes, simulations are restricted to a 5-path fading channel. For each signal to noise

Table I. Puncturing tables for the RCPT code with puncturing period $p = 4$ and information block size $N = 1024$

Code Rate	4/5	2/3	4/7	1/2	4/9	2/5	4/11	1/3
Puncturing patterm	16	17	17	17	17	17	17	17
	01	01	05	05	15	15	17	17
	01	01	01	05	05	15	15	17

ratio simulated in the plot, 10^4 information blocks and thus approximately 10^7 bits were simulated. No accepted packet errors were observed. From the plot, it is seen that the redundancy incremental Hybrid-ARQ (RCPT-ARQ) outperforms the simple Hybrid-ARQ with fixed rate RCPT codes in both cases, but the gain which is shown in Fig. 18 is rather small over a wide range of signal to noise ratios. As can be seen from Fig. 18, the throughput gain is less than 20% when the fading is quasi-static, and less than 10% when the fading is fast. Further from Fig. 17, it is seen that the simulated throughput curves are away from the ideal throughput curve by a certain amount of information rate due to the imperfection of the turbo code. There is also some jaggedness along the throughput curve under careful observations such as near the point SNR= $8dB$ for Hybrid-ARQ systems over a fast fading channel. Due to the large number of simulation samples, we can hypothesize that this jaggedness is the true reflection of the curve rather than simulation variations. Thus it is reasonable to predict that the curve will exhibit a "stairway-like" shape if the sampled SNR is dense enough. This is because the puncturing period adopted by the RCPT code is finite, which results in a limited number of available code rates (8 in our case).

Throughput for the same OFDM systems under time varying fading channels

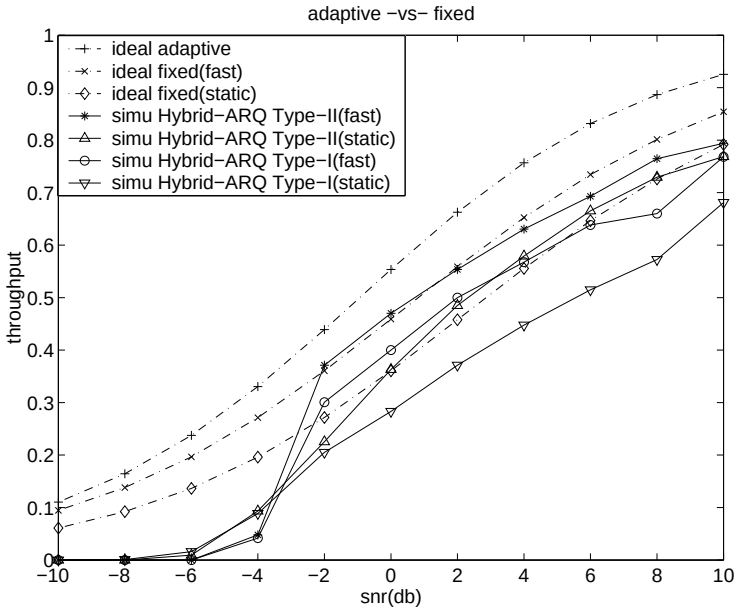

Fig. 17. Simulation throughput for Hybrid-ARQ (Type I) and redundancy incremental Hybrid-ARQ (Type II) OFDM systems

with different Doppler frequencies are illustrated in Fig. 19. The normalized Doppler frequency $f_d T_{frame}$ takes the OFDM frame period $T_{frame} = NT_s$ as a reference. As expected, all these throughputs are upper and lower bounded by the throughput of quasi-static fading channels and that of fast-fading channels.

The performance analysis of the throughput, which is given by (5.49) $\sim$ (5.58) in Section F, is illustrated and compared to the simulated throughput in Fig. 20. The critical capacity $C_{th}^{R_r}$ used in the above analysis was obtained by selecting the critical bit error probability p_{th} equal to 10^{-2} for quasi-static fading channels, and 0.5×10^{-2} for fast fading channels. From the plot, it is seen that the analysis can predict the throughput behavior over a wide range of signal to noise ratios, thus confirming the simulated loss from the ideal throughput curve.

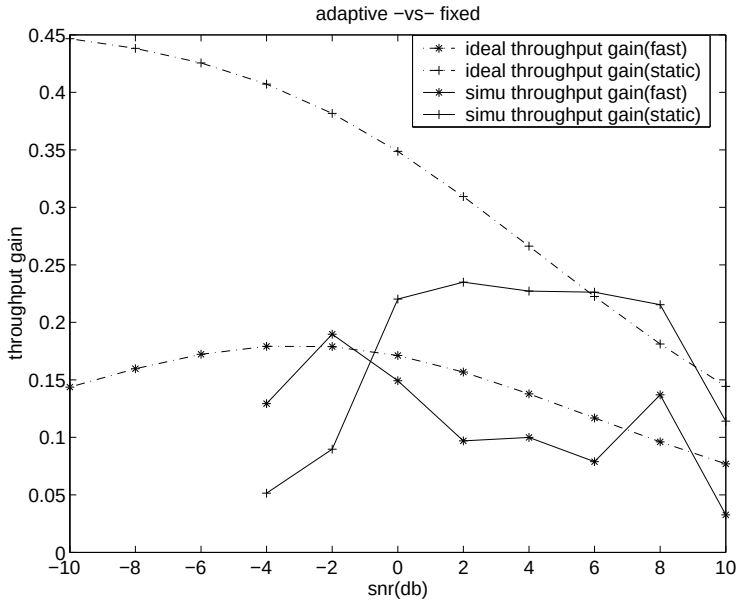

Fig. 18. Simulation throughput gain for Hybrid-ARQ (Type I) and redundancy incremental Hybrid-ARQ (Type II) OFDM systems

H. Conclusion on Resource Allocation

In this chapter, we have analyzed the power and rate allocations for the coded OFDM systems over frequency-selective fading environments. Taking an information theoretical point of view, the concept of instantaneous channel capacity was introduced and utilized as the building block of the system throughput analysis. Established as the ultimate limit for any OFDM system, the optimal throughput was compared with that of the uniform power and fixed rate allocation schemes under various channel conditions. After numerical evaluation of the analytical throughput was obtained, we reached the conclusion that over a wide range of signal to noise ratios, the throughput gain achieved by optimal water-filling power allocation and adaptive rate schemes is insignificant. Two practical OFDM systems implementing the Hybrid-ARQ and redundancy incremental Hybrid-ARQ schemes further verified limited throughput gain

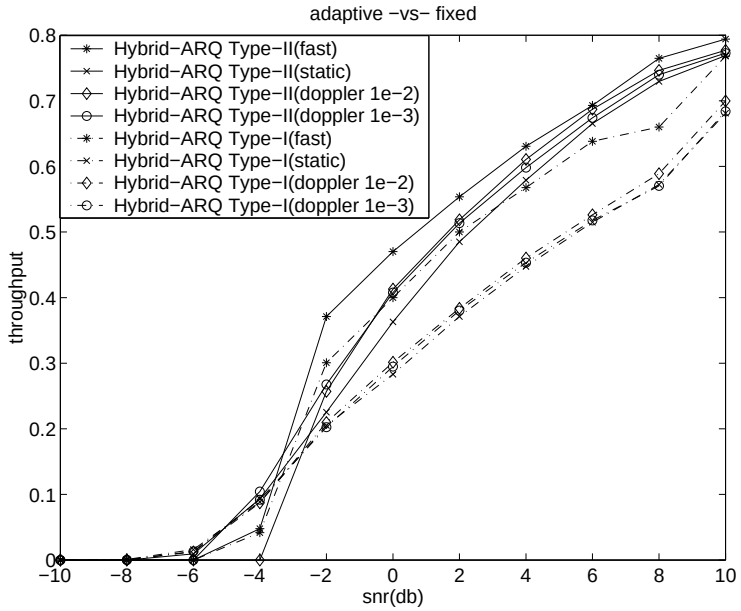

Fig. 19. Simulation throughput for Hybrid-ARQ (Type I) and redundancy incremental Hybrid-ARQ (Type II) OFDM systems under different fading rates (normalized Doppler frequency $f_d T_{frame} = 10^{-2}, 10^{-3}$)

through simulations and analysis.

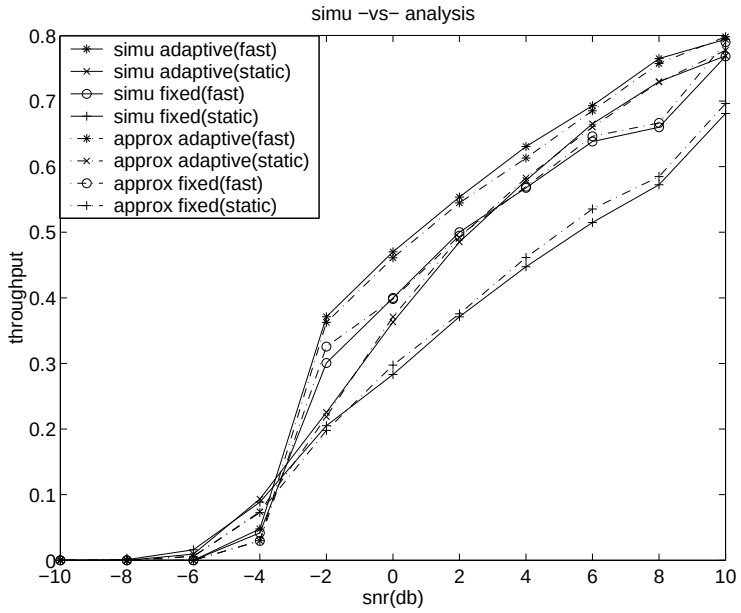

Fig. 20. Performance analysis of the throughput for Hybrid-ARQ (Type I) and redundancy incremental Hybrid-ARQ (Type II) OFDM systems

CHAPTER VI

SUMMARY

A. Performance Analysis of Coded OFDM Systems

In this thesis, performance analysis of coded OFDM systems over frequency-selective quasi-static fading channels are provided. Both the random coding upper bounds and the strong converse lower bounds are derived and shown to converge to the channel outage probability for large OFDM block lengths. Hence the outage probability is taken as the optimal performance indicator of a coded OFDM system and serves as a tool to compare with other communication systems operating in the same multi-path fading environment. Instead of evaluating the outage probability numerically, an approximate but analytically close form expression of the outage probability is provided.

B. Rate and Power Allocation of Coded OFDM Systems

In this thesis, we have also analyzed the power and rate allocations for the coded OFDM systems over frequency-selective fading environments. Taken from an information theoretical point of view, the concept of instantaneous channel capacity is implemented as the building block of the system throughput analysis. Established as the ultimate limit for any OFDM system, the optimal throughput was compared with that of the uniform power and fixed rate allocation schemes under various channel conditions. After numerical evaluation, we reached the conclusion that over a wide range of signal to noise ratios, the throughput gain achieved by optimal water-filling power allocation and adaptive rate schemes is insignificant. Two practical OFDM systems implementing the Hybrid-ARQ and redundancy incremental Hybrid-ARQ

schemes further verified limited throughput gain through simulations and analysis.

REFERENCES

[1] S. B. Weinstein and P. M. Ebert, "Data transmission by frequency-division multiplexing using the discrete Fourier transform," *IEEE Trans. Commun. Technol.*, vol. COM-19, pp. 628-634, Oct. 1971.

[2] J. A. C. Bingham, "Multicarrier modulation for data transmission: An idea whose time has come," *IEEE Commun. Mag.*, vol. 28, pp. 5-14, May 1991.

[3] B. Lu, X. Wang, and K. R. Narayanan, "LDPC-based space-time coded OFDM systems over correlated fading channels: Performance analysis and receiver design," *IEEE Trans. Wireless Commun.*, vol. 1, pp. 213-225, Apr. 2002.

[4] H. Kim, "Turbo coded orthogonal frequency division multiplexing for digital audio broadcasting," in *2000 IEEE Intern. Conf. on Commun.*, vol. 1, pp. 420-424.

[5] G. Yi, and K. B. Letaief, "Space-frequency-time coded OFDM for broadband wireless communications", in *2001 Global Telecommun. Conf.*, vol. 1, pp. 519-523.

[6] V. D. Nguyen, and H. -P. Kuchenbecker, "Block interleaving for soft decision Viterbi decoding in OFDM systems", in *2001 Vehicular Technology Conference*, vol. 1, pp. 470-474.

[7] E. Malkamaki and H. Leib, " Coded diversity on block-fading channels," *IEEE Trans. Inform. Theory*, vol. 45, pp. 771-781, Mar. 1999.

[8] R. G. Gallager, *Information Theory and Reliable Communication*. New York: Wiley, 1968.

[9] A. J. Viterbi and J. K. Omura, *Principles of Digital Communication and Coding.* Tokyo, Japan: McGraw-Hill, 1979.

[10] S. Arimoto, " On the converse to the coding theorem for discrete memoryless channels," *IEEE Personal Commun.*, vol. IT-19, pp. 357-359, May 1973.

[11] M. Ditzel, and W. A. Serdijn, "Optimal energy assignment for frequency selective fading channels", in *12th IEEE International Symposium on Personal, Indoor and Mobile Radio Communications*, vol. 1, pp. 104-108, 2001.

[12] A. Czylwik, "Adaptive OFDM for wideband radio channels," in *1996 Global Telecommun. Conf.*, vol. 1, pp. 713-718.

[13] N. Maeda, S. Sampei, and N. Morinaga, "A delay profile information based subcarrier power control combined with a partial non-power allocation technique for OFDM/FDD systems," in *11th IEEE International Symposium on Personal, Indoor and Mobile Radio Communications*, vol. 2, pp. 1380-1384, 2000.

[14] T. Yoshiki, S. Sampei, and N. Morinaga, "High bit rate transmission scheme with a multilevel transmit power control for the OFDM based adaptive modulation systems," in *2001 Vehicular Technology Conference*, vol. 1, pp. 727-731.

[15] K. -K. Wong, S. -K. Lai, R. S. -K. Cheng, K. B. Letaief, and R. D. Murch, "Adaptive spatial-subcarrier trellis coded MQAM and power optimization for OFDM transmissions," in *2000 Vehicular Technology Conference*, vol. 3, pp. 2049-2053.

[16] L. Piazzo, "Fast algorithm for power and bit allocation in OFDM systems," *Electronics Letters*, vol. 35, pp. 2173-2174, Dec 1999.

[17] J. G. Proakis, *Digital Communications,* 2nd ed., New York: McGraw-Hill, 1989.

[18] T. M. Cover and J. A. Thomas, *Elements of Information Theory.*, Wiley, New York, 1991.

[19] J. Zheng and S. L. Miller, "Performance analysis of coded OFDM systems over frequency-selective fading channels", accepted by *2003 Global Telecommun. Conf.*

[20] G. Ungerboeck, "Channel coding with multilevel/phase signals," *IEEE Trans. Inform. Theory*, vol. IT-28, no. 1, pp. 55-67, Jan 1982.

[21] A. Czylwik, "Kanalkapazitat von Breitband-Funkkanalen", *Klein-heubacher Berichte 39,* pp. 297-310, 1996.

[22] D. N. Rowitch and L. B. Milstein, "On the performance of hybrid FEC/ARQ systems using rate compatible punctured turbo (RCPT) codes", *IEEE Trans. on Comm.,* vol. 48, pp. 948 -959, Jun. 2000.

[23] D. Divsalar and F. Pollara, "Turbo codes for PCS applications," in *1995 IEEE Intern. Conf. on Comm.*, vol. 1, pp. 54-59, Jun. 1995.

[24] B. A. Harvey and S. B. Wicker, "Packet combining systems based on the Viterbi decoder," *IEEE Trans. on Comm.,* vol. 42, pp. 1544-1557, Feb./Mar./Apr. 1994.

[25] D. Chase, "Code combining – A maximum likelihood decoding approach for combining an arbitrary number of noisy packets," *IEEE Trans. on Comm.,* vol. 33, pp. 385-393, May 1985.

[26] D. Divsalar, "A simple tight bound on error probability of block codes with application to turbo codes," *TMO Progress Report,* pp. 42-139 Nov 15, 1999.

[27] T. Richardson and R. Urbanke, "An introduction to the analysis of iterative coding systems," *The IMA volumes in Mathematics and its Applications, (Codes, systems, and graphical models),* vol. 123, pp. 1-37, 2001.

[28] T. Richardson, A. Shokrohalli, and R. Urbanke, "Design of capacity approaching irregular low density parity check codes," *IEEE Trans. Inform. Theory,* vol. 47, pp. 619-637, Feb 2001.

[29] D. N. Rowitch, "Convolutional and turbo coded multicarrier direct sequence CDMA, and applications of turbo codes to hybrid ARQ communication systems," Ph.D. dissertation, Univ. of California at San Diego, La Jolla, June 1998.

APPENDIX A

CONDITIONAL SUB-CHANNEL CAPACITY

In this appendix, a derivation is provided for the approximate conditional sub-channel capacity $C(\gamma_i)$ given in (3.15). To begin it is noted that

$$\ln\cosh(y) = \ln\Big(\frac{\exp(-y)+\exp(y)}{2}\Big) = |y| + \ln\Big(\frac{1+\exp(-2|y|)}{2}\Big)\,. \tag{A.1}$$

Denote the second term in the above equation by

$$g(y) = \ln\Big(\frac{1+\exp(-2|y|)}{2}\Big)\,. \tag{A.2}$$

It can be approximated as an exponential function given by

$$\widehat{g}(y) = a\cdot\Big(\exp(-b\cdot|y|) - c\Big)\,, \tag{A.3}$$

where a, b and c are chosen such that

$$\widehat{g}(y)|_{y=0} = g(y)|_{y=0}\,, \tag{A.4}$$

$$\widehat{g}(y)'|_{y=0} = g(y)'|_{y=0}\,, \tag{A.5}$$

$$\widehat{g}(y)|_{y=\infty} = g(y)|_{y=\infty}\,. \tag{A.6}$$

By matching the approximation according to (A.5)-(A.6), $\widehat{g}(y)$ and $g(y)$ are forced to have the same origin, the same terminal, and the same first order derivative at the origin. After some straightforward calculus, we have

$$a = \ln 2, \qquad b = \frac{1}{\ln 2}, \qquad c = 1\,, \tag{A.7}$$

and thus

$$\ln\cosh(y) \approx |y| + \ln 2\cdot\Big(\exp(-\frac{|y|}{\ln 2}) - 1\Big)\,. \tag{A.8}$$

Plugging the approximation (A.8) into the definition of conditional sub-channel capacity in (3.12), we get

$$C(\gamma_i) \approx h(\gamma_i) = 1 - \frac{4\gamma_i}{k} Q(\sqrt{2\gamma_i}) - \exp\Big((k^2+2k)\gamma_i\Big) Q\Big((k+1)\sqrt{2\gamma_i}\Big) - \exp\Big((k^2-2k)\gamma_i\Big) Q\Big((k-1)\sqrt{2\gamma_i}\Big) - \frac{2\sqrt{\gamma_i}}{\sqrt{\pi}k} \cdot \exp(-\gamma_i), k = \frac{1}{\ln 2}. \quad \text{(A.9)}$$

Once again, the above formula can be approximated as an exponential function by

$$\widehat{h}(\gamma_i) = d - c \cdot \exp(-m\gamma_i)\,, \quad \text{(A.10)}$$

where d, c, and m are chosen following the same reasoning as (A.5)-(A.6), such that

$$\widehat{h}(\gamma_i)|_{\gamma_i=0} = 0\,, \quad \text{(A.11)}$$

$$\widehat{h}(\gamma_i)|_{\gamma_i=\infty} = 1\,, \quad \text{(A.12)}$$

$$\widehat{h}'(\gamma_i)|_{\gamma_i=\delta} = h'(\gamma_i)|_{\gamma_i=\delta}\,. \quad \text{(A.13)}$$

It then follows that

$$d = 1, \quad c = 1, \quad m = 1.24 \ (\delta = 0.2)\,, \quad \text{(A.14)}$$

$$C(\gamma_i) \approx 1 - \exp(-m\gamma_i)\,. \quad \text{(A.15)}$$

APPENDIX B

MEAN AND VARIANCE OF THE CONDITIONAL SUB-CHANNEL CAPACITY

Utilizing the approximation obtained in Appendix A, the mean and variance of the instantaneous channel capacity are evaluated in this appendix.

According to the definition, the instantaneous channel capacity is given by

$$C_N(\boldsymbol{\alpha}^{(t)}) = \frac{1}{N}\sum_{i=1}^{N} C(|\alpha_i^{(t)}|^2 \cdot \gamma_s) \ , \tag{B.1}$$

where γ_s is given by (5.22), and $|\alpha_i^{(t)}|$ follows a Rayleigh distribution given by (2.10) with variance $E[\,|\alpha_i^{(t)}|^2] = 1$. Plugging (A.15) in to the above equation,

$$E_{\alpha_i^{(t)}}\Big(C(|\alpha_i^{(t)}|^2 \cdot \gamma_s)\Big) \approx 1 - E_{\alpha_i^{(t)}}\Big(\exp(-m \cdot |\alpha_i^{(t)}|^2\gamma_s)\Big) = \frac{m\gamma_s}{1+m\gamma_s}\,. \tag{B.2}$$

Thus it is obvious that

$$\mu_{C_N} \approx \frac{m\gamma_s}{1+m\gamma_s}\,. \tag{B.3}$$

Applying the approximation (A.15) once again, the variance can be written as

$$\begin{aligned} E[C_N^2(\boldsymbol{\alpha}^{(t)})] \approx 1 &- \frac{2}{N}\sum_{i=1}^{N} E_{\alpha_i^{(t)}}\Big(\exp(-m \cdot |\alpha_i^{(t)}|^2\gamma_s)\Big) \\ &+\frac{1}{N^2}\sum_{i=1}^{N}\sum_{j=1}^{N} E_{\alpha_i^{(t)},\,\alpha_j^{(t)}}\left(\exp\Big(-m\cdot\Big(|\alpha_i^{(t)}|^2 + |\alpha_j^{(t)}|^2\Big)\cdot\gamma_s\Big)\right)\,. \end{aligned} \tag{B.4}$$

It is also straightforward to develop the following equation

$$\begin{aligned} &E_{\alpha_i^{(t)},\,\alpha_j^{(t)}}\left(\exp\Big(-m\cdot\Big(|\alpha_i^{(t)}|^2 + |\alpha_j^{(t)}|^2\Big)\cdot\gamma_s\Big)\right) \\ &\qquad = E_{\alpha_i^{(t)}}\left(\exp(-m\cdot|\alpha_i^{(t)}|^2\gamma_s)\cdot E_{\alpha_j^{(t)}/\alpha_j^{(t)}}\Big(\exp(-m\cdot|\alpha_j^{(t)}|^2\gamma_s)\Big)\right)\,. \end{aligned} \tag{B.5}$$

Conditioned on $\alpha_i^{(t)}$, $\alpha_j^{(t)}$ is still a complex Gaussian random variable with mean $\rho_{i,j}\alpha_i^{(t)}$ and variance $E(|\alpha_j^t|^2) = (1-\rho_{i,j}^2)$, where $\rho_{i,j}$ is the correlation coefficient. Thus $|\alpha_j^{(t)}|$

has a Rician distribution conditioned on $\alpha_i^{(t)}$. Using the characteristic function of the Rician distribution, the following expectation is obtained:

$$E_{\alpha_j^{(t)}/\alpha_i^{(t)}} \Big(\exp(-m \cdot |\alpha_j^{(t)}|^2 \gamma_s) \Big) = \frac{1}{1 + m(1 - |\rho_{i,j}|^2)\gamma_s} \cdot \exp\Big(- \frac{m\gamma_s(1 - |\rho_{i,j}|^2)|\rho_{i,j}|^2 |\alpha_i^{(t)}|^2}{1 + m\gamma_s(1 - |\rho_{i,j}|^2)} \Big) \ . \quad \text{(B.6)}$$

Plugging (B.6) into (B.5),

$$E_{\alpha_i^{(t)}, \alpha_j^{(t)}} \left(\exp\Big(- m \cdot \Big(|\alpha_i^{(t)}|^2 + |\alpha_j^{(t)}|^2 \Big) \cdot \gamma_s \Big) \right) = \frac{1}{(1 + m\gamma_s)^2 - (m\gamma_s)^2 \cdot |\rho_{i,j}|^2} \ . \quad \text{(B.7)}$$

From (2.6) and (2.7), the cross-correlation matrix of $\boldsymbol{\alpha}^{(t)}$ is given by the following format

$$\Sigma_{\alpha\alpha} = W_{N \times N} \cdot \Sigma_{cc} \cdot W_{N \times N}^H, \quad \Sigma_{cc} = \begin{pmatrix} I_{L \times L} & \mathbf{0} \\ \mathbf{0} & \mathbf{0} \end{pmatrix} / L \ . \quad \text{(B.8)}$$

After some calculus, the correlation coefficient between $\alpha_i^{(t)}$ and $\alpha_j^{(t)}$ is

$$|\rho_{i,j}| = \frac{1}{L} \cdot \frac{\sin\Big(L(i-j)\pi/N\Big)}{\sin\Big((i-j)\pi/N\Big)} \ . \quad \text{(B.9)}$$

Plugging (B.7) and (B.9) into (B.4), the variance of the instantaneous channel capacity can be represented as

$$\sigma_{C_N}^2 = E[C_N^2(\boldsymbol{\alpha}^{(t)})] - \mu_{C_N}^2 \approx \frac{1}{N} \sum_{k=0}^{N-1} \frac{1}{(1 + m\gamma_s)^2 - (m\gamma_s)^2 \cdot |r_k|^2} \ - \ \frac{1}{(1 + m\gamma_s)^2} \, , \quad \text{(B.10)}$$

where r_k is given by (5.36).

Applying a Taylor series expansion on (B.7), we have

$$\frac{1}{(1 + m\gamma_s)^2 - (m\gamma_s)^2 \cdot |r_k|^2} \approx \sum_{n=0}^{K} \frac{(m\gamma_s)^{2n}}{(1 + m\gamma_s)^{2n+2}} \cdot |r_k|^{2n} \, . \quad \text{(B.11)}$$

Plugging the partial Taylor series (B.11) into (B.10), the variance of the instantaneous channel capacity can be rewritten as

$$\sigma^2_{C_N} \approx \sum_{k=1}^{K} \frac{(m\gamma_s)^{2k}}{(1+m\gamma_s)^{2k+2}} \cdot \Big(\frac{1}{N}\sum_{n=0}^{N-1} |r_n|^{2k}\Big) \,. \tag{B.12}$$

Since the rectangular function $f[n]$ has a DFT given by

$$f[n] = (u[n] - u[n-L])/L \,, \tag{B.13}$$

$$\widehat{f}[k] = \frac{1}{L} \cdot \frac{\sin\Big(Lk\pi/N\Big)}{\sin\Big(k\pi/N\Big)} \cdot \exp\Big(-j\frac{(L-1)k\pi}{N}\Big) \,, \tag{B.14}$$

using the property of convolution and applying Parseval's formula, we can get

$$\sum_{n=0}^{N-1} |\underbrace{f \otimes f \cdots \otimes f[n]}_{k}|^2 = \frac{1}{N}\sum_{n=0}^{N-1} \Big(\frac{1}{L} \cdot \frac{\sin\left(Lk\pi/N\right)}{\sin\left(k\pi/N\right)}\Big)^{2k} = \frac{1}{N}\sum_{n=0}^{N-1} |r_n|^{2k} \,. \tag{B.15}$$

When $L \ll N$, which is a reasonable assumption for OFDM systems, the circular convolution between function $f[n]$ reduced to to the standard convolution. After straightforward calculus, Eq. (B.12) can be further simplified to be

$$\sigma^2_{C_N} \approx \sum_{k=1}^{K} \frac{(m\gamma_s)^{2k}}{(1+m\gamma_s)^{2k+2}} \cdot h_k(L) \,, \tag{B.16}$$

where $h_k(L)$ is given by (5.39), which is independent of N.

VITA

Jun Zheng was born in Hangzhou, Zhejiang, China. His permanent address is: Rm202, BLDG 14, HuaXianXinCun, Hangzhou, Zhejiang 310011, P.R.China. He graduated from Tsinghua University in 2001 with a B.S. in electrical engineering. From September 2001 to August 2003, he studied at Texas A& M University for his M.S. degree.

The typist for this thesis was Jun Zheng.